Doctoral Dissertation (Shinshu University)

Study on mechanical properties of polymeric latex films

高分子微粒子から成るフィルムの力学特性に関する研究

March 2021

Seina HIROSHIGE

Table of Contents

4. Summary

1. Introductory remarks

1.1. Background

1.1.1. Commonly Used Polymeric Materials

In general, synthetic polymeric materials that we use in our daily life can be divided into two groups based on the method used for their synthesis. One group comprises methods that utilize linear polymers (e.g., solution and bulk polymerization), while the other group contains polymers formed from methods that use polymer microspheres (e.g., emulsion, mini-emulsion, or precipitation polymerization). Polymeric materials formed from polymer microspheres, called latex films,[1-3] have found many every-day applications because they are able to form films in water systems, are easy to store, and are environmentally friendly. Latex films have found three major areas of applications in paints,[4,5] adhesives,[6,7] and paper processing,[8,9] and are also used as ink[10] for posters, signboards, and road markings. Because they are water-based materials with a low impact on the human body, they are also used in rubber gloves and cosmetics. In columns[11] and pressure sensors[12-14] they are used for the structural color change that is produced by the aggregation of the microspheres. Thus, it can be concluded that in our daily life, we are surrounded by a variety of synthetic polymeric materials formed from polymer microspheres.

1.1.2 The Disadvantages of Latex Films

Latex films tend to be brittle; accordingly, the polymeric materials formed from polymer microspheres described above require additives (impurities) and organic solvents to ensure sufficient strength of the films.[15] Thus, fusion auxiliaries that promote the fusion of the microspheres, cross-linking agents that tightly bind the interface of the microspheres, anti-aging agents, vulcanizing agents, and others are often introduced in such films (**Table 1**). However, the impact of these additives on the environment and human health are often problematic.

Table 1. Classification of the additives used in the preparation of films from polymer microspheres.

Additives	Function	Examples of additives
Cross-linkers	Cross-linked with microsphere interface	Colloidal sulfur, Zinc oxide, Vulcanization accelerator
Coalescing aids	Lower the film-formation temperature	Butyl glycol, Texanol
Viscous agents	Control the viscosity	Carboxymethyl cellulose, Polyvinylpyrrolidone, Bentonite
Wetting agents/dispersants	Stabilization of microsphere dispersion	Silicate, Lecithin, Acetylene tertiary alcohol
Fillers	Reinforce the films	Silicate, Lecithin, Silica particles, Carbon nanotubes

Polymer microspheres exhibit unique properties that are significantly different to those of linear polymers. Therefore, one of the factors that currently prevents the improvement of the mechanical properties of films made from polymer microspheres is the need to consider the preservation these unique properties. In addition to the toughness of the individual microspheres, films made from polymer microspheres need to take into account the deformation and bonding behavior of the microspheres, as well as the depth of the interpenetration of the polymer chains at the interface of the microspheres. Only when both factors are adequately considered can the mechanical properties of the film be improved.

1.1.3 Toughening of Materials

There are two main methods for toughening materials. The first method is to strengthen the material by forming a composit in a matrix. Important examples of this method includer reinforced concrete, invented in 1853, and carbon-fiber-reinforced plastics (**Table 2**). The secound method is to strengthen the material by focusing on the 'crosslink point' in network polymers. In recent years, it has been confirmed that various mechanical properties (such as high elongation, swelling, or elasticity), that cannot be attained by conventional cross-linking, can be importanted on a bulk polymer material by focusing on the 'crosslink point'. In 2002, Haraguchi *et al*. reported the synthesis of nanocomposite hydrogels via a radical polymerization in the presence of an *N*-isopropylacrylamide (NIPAm) monomer and silicate nanoplatelets.[16,17] These hydrogels showed high fracture strain (~1000%) and it was proposed that the brush-like polymers connect several silicate nanoparticles by physical cross-linking that is mainly a result of hydrogen bonding. In

addition, silica particles,[18,19] graphene oxide,[20] activated carbon,[21] and magnetic particles (iron oxide)[22] have been used in lieu of the clay. In 2003, Gong *et al*. reported strong hydrogels generated by inducing a double network structure from various combinations of hydrophilic polymers.[23-26] These double network hydrogels (DN gels) consist of a primary network (PAMPS: poly(2-acrylamido-2-methyl-propanesulfonic acid) and a secondary network (PAAm: polyacrylamides). When the DN gel is stressed, the primary network that is rigid and brittle breaks down. As this break occurs at various locations in the DN gel, the energy given to the gel by the stress is dissipated. Subsequently, the soft and flexible secondary network breaks down, which requires a certain degree of the spread of the rigid primary network. Thus, DN gels that the macroscopic rupture is suppressed is very tough. In 2008, Sakai *et al*. reported a tetra-PEG gel by combining two symmetric tetrahedron-like macromonomers of the same size.[27] These tetra-PEG gels exhibit good mechanical properties and a homogeneous structure, and are thus ideally suited networks to apply to model systems. [28,29]

In 1999, de Gennes proposed the general idea of a polymer chain cross-linked with cyclic molecules.[30] Such sliding gels were expected to exhibit different properties from chemically or physically cross-linked polymers. In fact, in 2001, Ito *et al*. synthesized cross-linked polymers wherein the polymer chain can move freely about the figure-of-eight-shaped cross-linking point.[31-35] Subsequently, Takata *et al*. synthesized a 'rotaxane crosslinker' that consists of a crown ether or cyclodextrin wheel and an axle that have vinyl group component.[36-44] It clarified that rotaxane cross-linker can be easily introduced into polymer materials. Thus, since 2000, the toughening of bulk polymeric materials has been achieved by focusing on the cross-linking of polymer chains.

Table 2. Examples of toughed materials.

Matrix	Composite materials	Products
Inorganic systems • Cement • Metals etc.	・Materials (reinforcing bar) ・Pozzolans ・Silica fumes ・Polymer materials	・Reinforced concrete ・High-strength concrete ・Blast furnace cement ・Silica cement
Organic systems • Natural rubbers • Synthetic rubbers • Gels • Plastics etc.	・Inorganic materials (e.g. carbon or silica particles, carbon nanotubes, glass fibers etc.) ・Peptizing agents ・Flexibilizers ・Age inhibitors	・Tires ・Seismic isolation rubbers ・Glass-fiber-reinforced-plastics ・Carbon-fiber-reinforced-plastics ・Boron-fiber-reinforced plastics ・Aramid-fiber-reinforced plastics
	Tough polymer materials focused on crosslinking structure • Nanocomposite hydrogels (NC gels) • Double network hydrogels (DN gels) • Tetra-PEG gels • Slide-ring gels etc.	

1.1.4 Focusing on surface/internal cross-linking of microspheres to form strong latex films

In recent years, much research has focused on the 'cross-linking structure' to toughen polymeric materials. To investigate whether it is possible to apply this research to microsphere films, which are widely used in an industrial context, we will focus on the surface and internal cross-linking of microspheres.

First, the surface crosslinking of microspheres will be examined. In order to provide greater strength, most conventional latex films used in industry are chemically cross-linked at the microsphere interface.[45-50] Chemical cross-linking of the surface improves the strength of the latex film, however, this also causes the latex film to become more hard and brittle. Therefore, this study focuses on the physical crosslinking at the microsphere interface via physical entanglement.

Next, the cross-linking structure inside the microspheres in an attempt to toughen latex films by applying rotaxane cross-link to the inside of the microspheres will be examined.

The synthesis of bulk materials with rotaxane cross-linked structures with a pulley effect was reported by Ito *et al*. in 2001. This approach has some disadvantages, such as a limited number of polymer chains to which it can be applied and a lack of structural details. This study will thus concentrate on a rotaxane molecule developed as a crosslinking agent. This crosslinking agent has a well-defined structure (one ring is introduced for one axis) and is capable of radical

polymerization with various vinyl groups. This cross-linker was employed in an attempt to improve film properties by changing the cross-linked structure inside the particles.

Chapter 1 focuses on the glass-transition temperature (T_g) of latex microspheres copolymerized with two different monomers and the minimum film-formation temperature (MFFT) of latex films. These parameters have emerged as key factors that microspheres deformation are controlled, and are expected to have strong correlation with the mechanical strength of the resulting latex films. **In Chapter 2**, the structure of the cross-links in the microspheres is examined. This is one of the important parameters influencing the mechanical properties of the microsphere films that was investigated.

1.2. References

[1] Joseph L. Keddie, Film formation of latex, *Material Science and Engineering*, 21,101-170, **1997**.

[2] P.A. Stewarda, J. Hearna, M. C. Wilkinson, An overview of polymer latex film formation and properties, *Advances in Colloid and Interface Science*, 86, 195-267, **2000**.

[3] J. L. Keddie, A. F. Routh, Fundamentals of Latex of Latex Film Formation Processes and Properties, *Springer*, **2010**.

[4] Lambourne, R. and Strivens, T. A. Paint and Surface Coatings. *Woodhead Publishing Ltd.*, **1999**.

[5] Liu, M. Mao, X. Zhu, H. Lin, A. Wang, D. Water and Corrosion Resistance of Epoxy–Acrylic–Amine Waterborne Coatings: Effects of Resin Molecular Weight, Polar Group and Hydrophobic Segment. *Corros. Sci.,* 75, 106–113, **2013**.

[6] Calvo, M. E. Míguez, H. Flexible, Adhesive, and Biocompatible Bragg Mirrors Based on Polydimethylsiloxane Infiltrated Nanoparticle Multilayers. *Chem. Mater.*, 22, 3909–3915, **2010**.

[7] N. Sato, A. Murata, T. Fujie, S. Takeoka, Stretchable, adhesive and ultra-conformable elastomer thin films, *Soft Matter*, 12, 9202, **2016**.

[8] Sababi, M. Kettle, J. Rautkoski, H. Claesson, P. M. Thormann, E. Structural and Nanomechanical Properties of Paperboard Coatings Studied by Peak Force Tapping Atomic Force Microscopy. *ACS Appl. Mater. Interfaces*, 4, 5534−5541, **2012**.

[9] J.-H. Lee, H. L. Lee, Characterization of the Paper Coating Structure Using Focused Ion Beam and Field-Emission Scanning Electron Microscopy. 2. Structural Variation Depending on the Glass Transition Temperature of an S/B Latex, *Ind. Eng. Chem. Res.* 57, 16718−16726, **2018**.

[10] S. Jiang, A. V. Dyk, A. Maurice, J. Bohling D. Fasanoc, S. Brownell, Design colloidal particle morphology and self-assembly for coating applications, *Chemical Society Reviews*, 46, 3792-3807, **2017**.

[11] Marchetti, P. Mechelhoff, M. Livingston, A. G. Tunable-Porosity Membranes from Discrete Nanoparticles. *Sci. Rep.*, 5, 17353, **2015**.

[12] Viel, B. Ruhl, T. Hellmann, G. P. Reversible Deformation of Opal Elastomers. *Chem. Mater.*, 19, 5673–5679, **2007**.

[13] Schäfer, C. G. Smolin, D. A. Hellmann, G. P. Gallei, M. Fully Reversible Shape Transition of Soft Spheres in Elastomeric Polymer Opal Films. *Langmuir*, 29, 11275–11283, **2013**.

[14] Ito, T. Katsura, C. Sugimoto, H. Nakanishi, E. Inomata, K. Strain-Responsive Structural Colored Elastomers by Fixing Colloidal Crystal Assembly. *Langmuir*, 29, 13951–13957, **2013**.

[15] J. W. Taylor, M. A. Winnik. Functional latex and thermoset latex films, *J. Coat. Technol. Res.*, *1*, 163-190, **2004**.

[16] K. Haraguchi, T. Takehisa, Nanocomposite Hydrogels: A Unique Organic–Inorganic Network Structure with Extraordinary Mechanical, Optical, and Swelling/De-swelling Properties**, *Adv. Mater.*, 14, 1120-1124, **2002**.

[17] K. Haraguchi, H. J. Li, Mechanical Properties and Structure of Polymer-Clay Nanocomposite Gels with High Clay Content, *Macromolecules*, 39, 1898-1905, **2006**.

[18] A. K. Gaharwar, C. P. Rivera, C. J. Wu, G. Schmidt, Transparent, elastomeric and tough hydrogels from poly(ethylene glycol) and silicate nanoparticles, *Acta Biomater.*, 7, 4139–4148, **2011**.

[19] T. Wei, L. J. Lei, H. L. Kang, B. Qiao, Z. Wang, L. Q. Zhang, P. Coates, K. C. Hua, J. Kulig, Tough Bio-Based Elastomer Nanocomposites with High Performance for Engineering Applications†, *Adv. Eng. Mater.*, 14, 112–118, **2012**.

[20] R. Q. Liu, S. M. Liang, X. Z. Tang, D. Yan, X. F. Li, Z. Z. Yu, Tough and highly stretchable graphene oxide / polyacrylamide nanocomposite hydrogels†, *J. Mater. Chem.*, 22, 14160–14167, **2012**.

[21] X. H. Liu, B. He, Z. P. Wang, H. F. Tang, T. Su, Q. G. Wang, Tough Nanocomposite Ionogel-based Actuator Exhibits Robust Performance, *Sci. Rep*. 4, 6673, **2014**.

[22] H. Haider, C. H. Yang, W. J. Zheng, J. H. Yang, M. X. Wang, S. Yang, M. Zrinyi, Y. Osada, Z. G. Suo, Q. Q. Zhang, J. X. Zhou, Y. M. Chen, Exceptionally tough and notch-insensitive magnetic hydrogels, *Soft Matter*, 11, 8253–8261, **2015**.

[23] J. P. Gong, Y. Katsuyama, T. Kurokawa, Y. Osada, Double-Network Hydrogels with Extremely High Mechanical Strength, *Adv. Mater*., 15, 1155–1158, **2003**.

[24] J. P. Gong, Materials both Tough and Soft, *Science*, 344, 161–162, **2014**.

[25] T. Matsuda, R. Kawakami, R. Namba, T. Nakajima, J.P. Gong, Mechanoresponsive self-growing hydrogels inspired by muscle training, *Science*, 363, 504–508, **2019**.

[26] T. Nakajima, Y. Tanaka, H. Furukawa, T. Kurokawa, J. P. Gong, Creation of Double Network Hydrogels with Extremely High Strength and Its Anomalous Fracture Mechanism, *Kobunshi Ronbunshu*, 65, 707–715, **2008**.

[27] T. Sakai, T. Matsunaga, Y. Yamamoto, C. Ito, R. Yoshida, S. Suzuki, N. Sasaki, M. Shibayama, U. I. Chung, Design and Fabrication of a High-Strength Hydrogel with Ideally Homogeneous Network Structure from Tetrahedron-like Macromonomers, *Macromolecules*, 41, 5379-5384, **2008**.

[28] T. Sakai, M. Kurakazu, Y. Akagi, M. Shibayama, U. Chung, Effect of swelling and deswelling on the elasticity of polymer networks in the dilute to semi-dilute region, *Soft Matter*, 8, 2730–2736, **2012**.

[29] T. Sakai, Experimental verification of homogeneity in polymer gels, *Polym. J.*, 46, 517–523, **2014**.

[30] P. G. de Gennes, Sliding gels, *Physica A*, 271, 231–237, **1999**.

[31] Y. Okumura, K. Ito, The Polyrotaxane Gel: A Topological Gel by Figure-of-Eight Cross-links, *Adv. Mater.* 13, 485–487, **2001**.

[32] K. Ito, Novel Cross-Linking Concept of Polymer Network: Synthesis, Structure, and Properties of Slide-Ring Gels with Freely Movable Junctions, *Polym. J.* 39, 489–499, **2007**.

[33] T. Karino, M. Shibayama, K. Ito, Slide-ring gel: Topological gel with freely movable cross-links, *Phys. B*, 385, 692–696, **2006**.

[34] N. Murata, A. Konda, K. Urayama, T. Takigawa, M. Kidowaki, K. Ito, Anomaly in stretching-induced swelling of slide-ring gels with movable cross-links, *Macromolecules*, 42, 8485–8491, **2009**.

[35] T. Arai, K. Jang, Y. Koyama, S. Asai, T. Takata, Versatile Supramolecular Cross-Linker: A Rotaxane Cross-Linker That Directly Endows Vinyl Polymers with Movable Cross-Links, *Chem. Eur. J.*, 19, 5917–5923, **2013**.

[36] K. Iijima, D. Aoki, H. Sogawa, S. Asai, T. Takata, Synthesis and characterization of supramolecular cross-linkers containing cyclodextrin dimer and trimer, *Polym. Chem*. 7, 3492–3495. **2016**.

[37] K. Iijima, D. Aoki, H. Otsuka, T. Takata, Synthesis of rotaxane cross-linked polymers with supramolecular cross-linkers based on γ-CD and PTHF macromonomers: The effect of the macromonomer structure on the polymer properties, *Polymer*, 128, 392–396, **2017**.

[38] K. Jang, K. Iijima, Y. Koyama, S. Uchida, S. Asai, T. Takata, Synthesis and properties of rotaxane-cross-linked polymers using a double-stranded γ-CD-based inclusion complex as a supramolecular cross-linker, *Polymer*, 128, 379–385, **2017**.

[39] M. Ogawa, A. Kawasaki, Y. Koyama, T. Takata, Synthesis and properties of a polyrotaxane network prepared from a Pd-templated bis-macrocycle as a topological cross-linker, *Polym. J.*, 43, 909–915, **2011**.

[40] M. Ogawa, H. Sogawa, Y. Koyama, T. Takata, Synthesis of rotaxane cross-linked polymers derived from vinyl monomers using a metal-containing supramolecular cross-linker, *Polym. J.*, 47, 580–584, **2015**.

[41] K. Iijima, Y. Kohsaka, Y. Koyama, K. Nakazono, S. Uchida, S. Asai, T. Takata, Stimuli-degradable cross-linked polymers synthesized by radical polymerization using a size-complementary [3]rotaxane cross-linker, *Polym. J.,* 46, 67–72. **2014**.

[42] J. Sawada, D. Aoki, S. Uchida, H, Otsuka, T. Takata, Synthesis of Vinylic Macromolecular Rotaxane Cross-Linkers Endowing Network Polymers with Toughness, *ACS Macro Lett*., 4, 598–601, **2015**.

[43] J. Sawada, D. Aoki, T. Takata, Vinylic Rotaxane Cross-Linker Comprising Different Axle Length for the Characterization of Rotaxane Cross-linked Polymers, *Macromol. Symp.*, 372, 115–119, **2017**.

[44] J. Sawada, D. Aoki, H. Otsuka, T. Takata, A Guiding Principle for Strengthening Crosslinked Polymers: Synthesis and Application of Mobility-Controlling Rotaxane Crosslinkers, *Angew. Chem. Int. Ed.*, 58, 2765-2768, **2019**.

[45] J. Hu, K. Peng, J. Guo, D. Shan, G. B. Kim, Q. Li, E. Gerhard, L. Zhu, W. Tu, W. Lv, M. A. Hickner and J. Yang, Click Cross-Linking-Improved Waterborne Polymers for Environment-Friendly Coatings and Adhesives, *ACS Appl. Mater. Interfaces*, 8, 17499–17510, **2016**.

[46] W. J. Soer, W. H. Ming, C. E. Koning, R. van Benthem, Crosslinking systems and film properties for surfactant-free latexes based on anhydride-containing polymers, *Polymer*, 49, 3399–3412, **2008**.

[47] M. D. Soucek, E. P. Pedraza, Control of functional site location for thermosetting latexes, *J. Coat. Technol. Res.* 6, 27–36, **2009**.

[48] H. Bakhshi, M. J. Zohuriaan-Mehr, H. Bouhendi, K. Kabiri, Effect of functional monomer GMA on the physical–mechanical properties of coatings from poly(BA–MMA) latexes, *J. Mater. Sci.* 46, 2771–2777, **2011**.

[49] H. H. Pham, M. A. Winnik, Polymer Interdiffusion vs Cross-Linking in Carboxylic Acid-Carbodiimide Latex Films. Effect of Annealing Temperature, Reactive Group Concentration, and Carbodiimide Substituent, *Macromolecules*, 39, 1425–1435, **2006**.

[50] W. Wohlleben, F. W. Bartels, M. Boyle, R. J. Leyrer, Covalent and Physical Cross-Linking of Photonic Crystals with 10-Fold-Enhanced Chemomechanical Stability, *Langmuir*, 24, 5627–5635, **2008**.

2. Chapter I

" Temperature-dependent Relationship between the Structure and Mechanical Strength of Volatile Organic Compound-free Latex Films Prepared from Poly(butyl acrylate-*co*-methyl methacrylate) Microspheres"

*Part of this work was published in "Seina Hiroshige, Haruka Minato, Yuichiro Nishizawa, Yuma Sasaki, Takuma Kureha, Mitsuhiro Shibayama, Kazuya Uenishi, Toshikazu Takata, and Daisuke Suzuki *Polymer Journal*, **2020**, *in press*." Reprinted with permission from Copyright (2020).
DOI: https://doi.org/10.1038/s41428-020-00406-6

2.1. Introduction

Latex consists of nano- to micrometer sized polymeric microspheres dispersed in an aqueous solution.[1,2] Latex films can be obtained by evaporating water from dispersions of water-borne latex microspheres in the absence of volatile organic compounds (VOCs), which is advantageous for the production of eco-friendly and human-body-friendly materials.[3,4] Therefore, such latex films are used widely not only in industrial applications, e.g., paints, [5,6] adhesives,[7,8] and paper coatings, [9,10] but also in next-generation advanced materials, e.g., strain-responsive structural colored elastomers,[11-13] biomaterial coatings,[14] porous membranes,[15] and hydrogel thin films with structural color.[16-19]

However, the mechanical strength of latex films that consist only of latex microspheres is poor due to their poor resistance to fracture between neighboring microspheres.[20,21] Many formation methods to improve the mechanical strength of latex films have been reported.[20] Most of these involve the introduction of additives. For example, neighboring latex microspheres have been cross-linked via post-polymerization reactions using additives such as chemical cross-linkers or reactive surfactants[22-24] during the dispersion-drying process. A method in which soft and hard latex microspheres are mixed has also been reported; the deformation of the soft microspheres decreases the voids between the hard microspheres.[25-27] Coalescing aids have also been used during the drying process to deform the microspheres and obtain a homogeneous nonporous latex film.[28-30] However, phase separation between the microspheres and additives may negatively affect the mechanical properties of the latex films and decrease film performance (e.g., aging deterioration[29]). Although many additive-based methods to improve the mechanical properties of

latex films have been developed, to the best of the author knowledge, methods using additive-free systems have not yet been reported.

In the present study, in order to clarify the relationship between the (nano)structure of latex films and their mechanical properties with the aim to obtain tougher latex films, I focused on the glass-transition temperature (T_g) of latex microspheres with different chemical structures and the minimum film-formation temperature (MFFT) of latex films. These parameters have emerged as important factors that control the deformation of the microspheres, which is expected to be strongly correlated with the mechanical properties of the resulting latex films. Through careful evaluation of the mechanical properties and the nanostructures of latex films using microscopy and scattering, I have closely examined this relationship.

2.2. Experimental Section

Materials

Methyl methacrylate (MMA, 98%), *n*-butyl acrylate (BA, 98%), and potassium peroxodisulfate (KPS, 95%) were purchased from FUJIFILM Wako Pure Chemical Corporation (Japan) and used as received. Sodium dodecyl benzene sulfonate (DBS, 95%) and *n*-hexadecane (HD, 97%) were purchased from Tokyo Chemical Industry Co., Ltd. (Japan) and used as received. Distilled and ion-exchanged water was used in all reactions, including the preparation of solutions and the purification of polymers (EYELA, SA-2100E1).

Synthesis and Characterization of the Microspheres

All elastomer microspheres used in this study were prepared using a mini-emulsion polymerization technique.[31] In all cases, the initial total monomer concentration was 1.6 M; the mixing ratio of the monomers (i.e., BA and MMA) was adjusted to modify the glass-transition temperature (T_g; polyBA: -46 °C; polyMMA: 102 °C) of the microspheres. An oil mixture of the monomers (BA and/or MMA; cf. Table 1) and HD (0.46 g) was suspended in water (30 mL) containing the anionic surfactant DBS (0.1 g). The suspension was subsequently homogenized via ultrasonication (3 min, 375 W) in an ice bath using an ultrasonic homogenizer (VC-75, SONICS). The suspension was then transferred into a four-necked round-bottom flask (50 mL) equipped with a mechanical stirrer, condenser, and nitrogen gas inlet. The solution was heated to 70 °C under a stream of nitrogen and constant stirring (200 rpm). After the solution had been sparged with nitrogen for at least 30 min,

the free-radical polymerization was initiated by adding the water-soluble anionic initiator KPS (0.1 g) dissolved in deionized water (6 mL). The reaction was stirred for 4 h, after which the dispersion was cooled to room temperature to stop the polymerization. The obtained elastomer microspheres were purified twice by centrifugation–redispersion in deionized water using a relative centrifugal force (RCF) of 20,000 *g* to remove unreacted reagents and other impurities, followed by dialysis using cellulose tubing in deionized water for a week, during which the water was changed on a daily basis. Hereafter, the obtained poly(BA-*co*-MMA) microspheres are denoted as B*X*M*Y*, where *X* represents the amount of BA monomer (mol %) and *Y* represents the amount of MMA monomer (mol %).

Characterization of the Latex Microspheres

The hydrodynamic diameter, D_h, of the obtained elastomer microspheres was determined using dynamic light scattering (DLS, Malvern Instruments Ltd., Zetasizer Nano S). The diameters of the microspheres were calculated based on the measured diffusion coefficients using the Stokes−Einstein equation (Zetasizer software v6.12). The time-average intensity correlation function was measured using 1 mL of a 0.001 wt% elastomer microsphere dispersion with a measurement time of 30 s. The zeta potential of the microspheres was calculated using a Zetasizer Nano ZS instrument (Malvern Instruments Ltd.) at a concentration of ~0.001 wt%. The obtained electrophoretic mobilities were analyzed by applying the Smoluchowski equation. Prior to the DLS and the zeta potential measurements, the samples were allowed to equilibrate for 10 min at 25 °C. In addition, the morphology of the individual latex microspheres was observed using field-emission scanning electron microscopy (FE-SEM, S-5000, Hitachi Ltd.). To prepare the FE-SEM sample, a microsphere dispersion (~0.1 wt%) was dried on a polystyrene substrate at room temperature; the substrate was then sputtered with Pt/Pd (15 mA, 6 Pa, 80 s). The size of the microspheres was measured from the FE-SEM images using the software package ImageJ (version 1.52a; Wayne Rasband, National Institutes of Health) (N = 50).

Evaluation of the T_g of the Elastomer Microspheres

The T_g of the microspheres was evaluated using differential scattering calorimetry (DSC, DSC-60, SHIMADZU Co. Ltd.); for that purpose, samples were heated from -60 °C to 150 °C at 10 °C/min. The T_g of the microspheres was determined by drawing tangents to the heat flow curve at

temperatures above and below T_g; the point of intersection of the bisector of the angle between the tangents with the measurement curve was used as the T_g.

Formation of Latex Films

Latex films were obtained by depositing an elastomer microsphere dispersion (2.4 mg microspheres in ~350 μL dispersion, which is enough to conduct the reliable tensile test) on a silicon rubber sheet (ISO 37-4 dumbbell-shaped specimen; 12 mm × 2 mm for tensile tests, 10 mm × 10 mm for small-angle X-ray scattering (SAXS) measurements), followed by drying at 10, 25, 40, or 70 °C for 24 h. The obtained films were annealed at 70 °C for varying periods of time (0, 18, 24, 72, 94 and 120 hours). Hereafter, the latex films prepared from B40M60 microsphere dispersions are denoted as F-B40M60-*Z*, whereby *Z* represents the FFT.

Characterization of the Latex Films

The morphology of the surfaces of the latex films was observed using an atomic force microscope (AFM, SPM-9500J3, Hitachi Ltd.) and FE-SEM. The surface of the latex films was sputtered with Pt/Pd prior to the FE-SEM observation (15 mA, 6 Pa, 80 s). The microscopic structures of the latex films were characterized using SAXS measurements at the BL03XU beam line of SPring-8 (Japan),[33] using an X-ray wavelength of 1.0 Å and a sample-to-detector distance of 4.0 m. The latex films were placed in the sample holder using Kapton tape. All the tested films were irradiated with the X-ray beam for 30 s under vacuum. To obtain one-dimensional scattering profiles, the two-dimensional images were integrated circularly using the program FIT2D. Tensile tests were performed at 25 °C using a testing machine (tensilonRTC1250A, A&D Company) equipped with a 50 N load cell at an elongation rate of 10 mm/min. The fracture energy of the latex films was determined by integrating the stress–strain curve.

2.3. Results and discussion

Synthesis and Characterization of the Microspheres.

First, to investigate the effect of the T_g of the microspheres on the morphology and mechanical properties of the latex films, a series of poly(BA-*co*-MMA) microspheres were synthesized using mini-emulsion polymerization.[31] The mini-emulsion polymerization technique was selected because this method enables the encapsulation of water-immiscible functional molecules such as

rotaxane crosslinkers,[31] which will be required for the subsequent experiments. The feed ratios of BA and MMA are shown in Table 1. Aggregation was not observed among any of the microspheres after polymerization, and the D_h values measured using DLS were ~100 nm, irrespective of the feed ratio of BA and MMA (Table 1). This result suggests that the mini-emulsion polymerization proceeded successfully, i.e., the oil droplets were transformed into microspheres after the polymerization.[34] Additionally, the zeta potential values were negative for all microspheres (Table 1) due to the use of the initiator KPS. It should be noted here that no impurities, e.g., the DBS used in the polymerization, remained after careful purification of the microspheres via dialysis and centrifugation, as was confirmed by a previously reported X-ray photoelectron spectroscopy analysis.[33] Moreover, the T_g of each microsphere composition was determined from the DSC curves shown in Figure 1. As expected, the T_g increased with increasing MMA ratio in the feed.

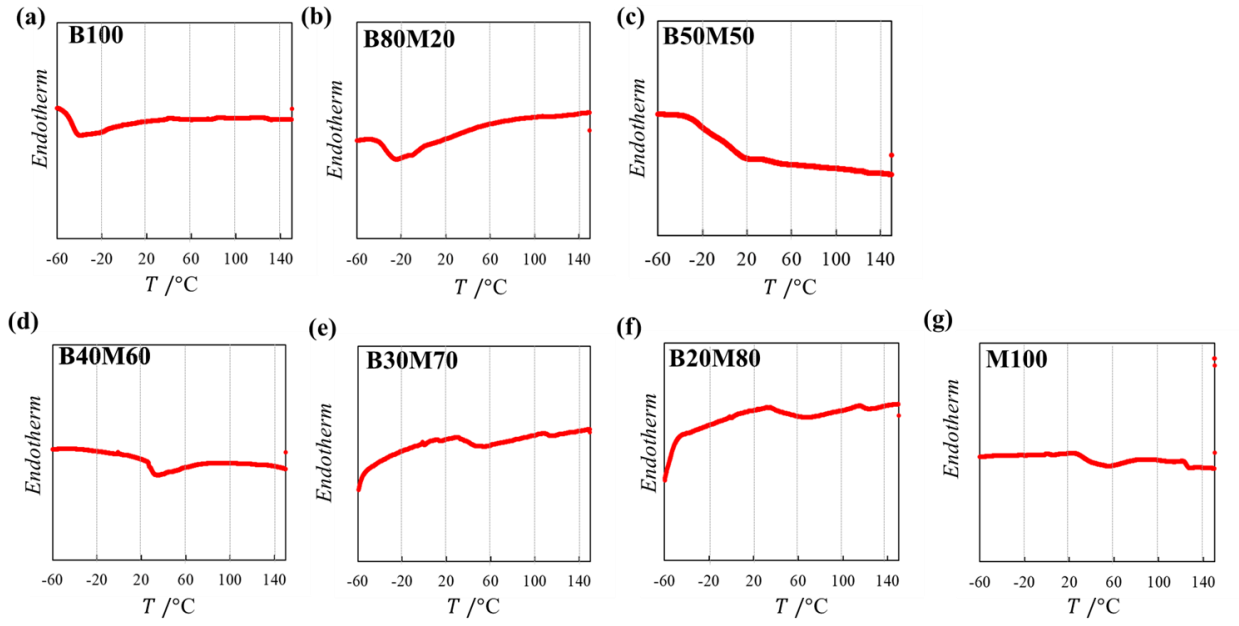

Figure 1. DSC curves of the **(a) B100**, **(b) B80M20**, **(c) B50M50**, **(d) B40M60**, **(e) B30M70**, **(f) B20M80**, and **(g) M100** microspheres.
(a), (d), and (g) were reproduced with permission from ref 2. Copyright (2019) Journal of Society of Rheology, Japan.

Furthermore, the shape and size of individual microspheres were evaluated using FE-SEM in the dried state (Figure 2). The shapes of the B100, B80M20, B50M50, and B40M60 microspheres, which contain high percentages of BA, could not be observed, because the microspheres were too soft at the observation temperature (~25 °C). In other words, although the microspheres with T_g

values below room temperature can be stably dispersed in water due to their surface charge, these microspheres coalesce and undergo deformation in the dried state. On the other hand, the microspheres with high MMA contents and T_g values above room temperature are spherical with average diameters of 97 ± 10 nm (B30M70), 91 ± 10 nm (B20M80), and 59 ± 6 nm (M100) (Figure 2), which are values similar to those determined by DLS.

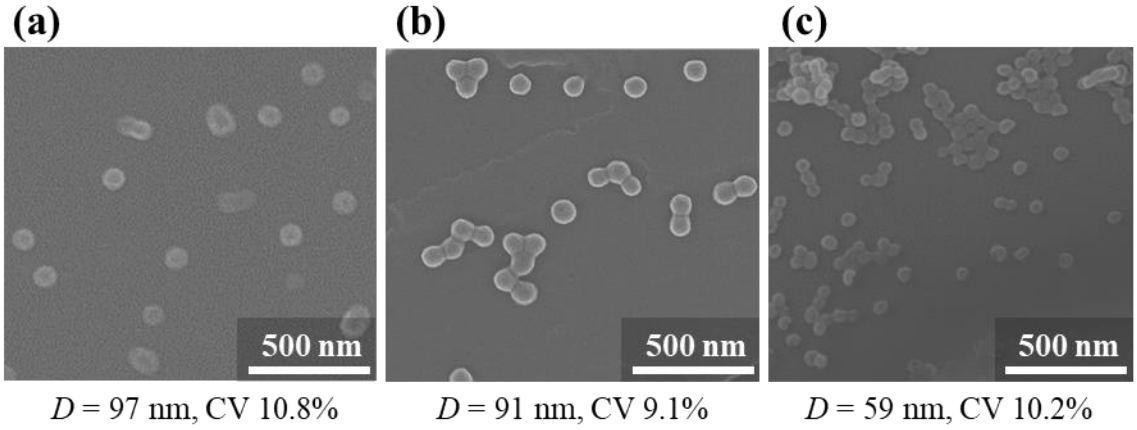

Figure 2. FE-SEM images of **(a) B30M70**, **(b) B20M80**, and **(c) M100** microspheres. The dispersions (0.1 wt%) were dried at room temperature on a polystyrene substrate.

Table 1. Chemical composition and properties of the poly(BA-*co*-MMA) microspheres prepared by mini-emulsion polymerization.

Sample	Monomers		D_h	Zeta potential	T_g
	BA (mol%)	MMA (mol%)	(nm)	(mV)	(°C)
B100	100 (7.4 g)	–	147±1.6	−32.8	-51
B80M20	80 (5.9 g)	20 (1.2 g)	113±0.3	−54.9	-39
B50M50	50 (3.7 g)	50 (2.3 g)	100±0.7	−50.9	-11
B40M60	40 (3.0 g)	60 (3.5 g)	94.8±1.3	−46.1	24
B30M70	30 (2.2 g)	70 (4.6 g)	92.1±0.4	−45.6	35
B20M80	20 (1.5 g)	80 (4.8 g)	141±1.2	−51.0	65
M100	–	100 (5.8 g)	94.8±0.7	−39.4	124

Preparation of Latex Films Composed of Poly(BA-*co*-MMA) Microspheres

Next, a series of latex films was formed via evaporation of water from the obtained dispersions. In my previous study, I confirmed that B40M60 microspheres can form a self-standing latex film

after the evaporation of water,[31] while microspheres with different BA/MMA comonomer ratios (i.e., B100, B80M20, B50M50, B30M70, and M100) did not form self-standing films at room temperature. [31] Self-standing latex films can be obtained when dispersions are dried above the minimum film-formation temperature (MFFT), which is approximately equal to the T_g of the microspheres.[30] Therefore, the author re-examined the film-formation ability of the microspheres with different comonomer ratios by changing the drying temperature systematically. Figure 4 summarizes the latex-film-formation results using the microspheres shown in Table 1 at different drying temperatures. The B40M60 microspheres formed self-standing latex films at all the tested FFTs except for 4 °C; although the film formed at 4 °C (FFT<<T_g) was free-standing, it was brittle and broke (Figure 3), suggesting that the degree of microsphere deformation during the evaporation of the dispersion is insufficient when the FFT is much lower than the T_g of the microspheres. As expected, the microspheres with higher MMA ratios, i.e., B30M70, B20M80, and M100, did not form latex films that maintained the shape of the mold at 4 °C (Figure 3). With increasing MMA ratio, the minimum FFT where self-standing latex films were obtained also increased, and the microspheres with the highest MMA ratio (M100) failed to produce a self-standing film at any of the measured FFTs (Figure 3, Figure 4). On the other hand, the microspheres with a slightly higher BA ratio than B40M60, i.e., B50M50, formed a self-standing latex film at 4 °C. The B80M20 and B100 microspheres formed latex films at 4 °C, but the films were too soft to be self-standing after being removed from the mold (Figure 3). With increasing BA ratio in the microspheres, the latex films were not self-standing at even lower FFT (Figure 4, Figure 3), suggesting that the softness of the microspheres, i.e., their deformability, is an important factor in the formation of self-standing latex films. These results confirm that rigid species such as MMA are crucial for the formation of self-standing elastomers from microspheres, as has previously been reported for poly(BA-*co*-MMA) microspheres prepared by emulsion polymerization.[35]

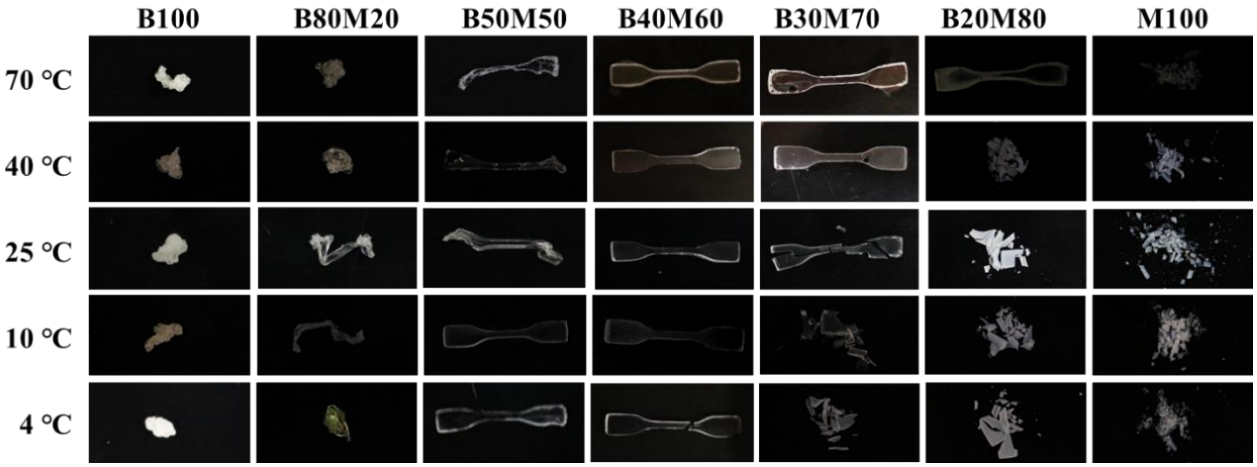

Figure 3. Photographs of latex films prepared by depositing **B*X*M*Y*** (BA: ***X*** mol%; MMA: ***Y*** mol%) elastomer microsphere dispersions on a silicon rubber sheet (ISO 37-4 dumbbell-shaped specimen 12 mm × 2 mm), followed by drying at 4 °C, 10 °C, 25 °C, 40 °C, or 70 °C.

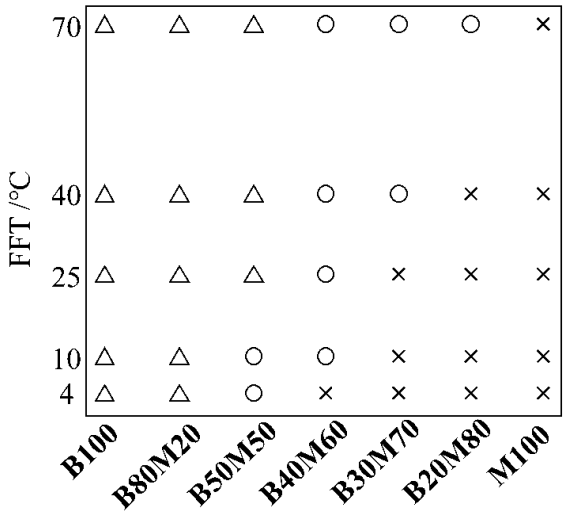

Figure 4. Phase diagram of films formed using aqueous dispersions of the various poly(BA-*co*-MMA) microspheres at different drying temperatures. Circles (○) indicate that a free-standing latex film was formed. Triangles (△) indicate that a film was formed that was not self-standing after removal from the mold. Crosses (×) indicate that a film was not formed. Photographs of each film are shown in **Figure 3.**

Characterization of the Latex Films Prepared from Poly(BA-*co*-MMA) Microspheres

To characterize the morphology of all the evaporated microsphere dispersions, even those that did not form self-standing latex films, droplets containing the microspheres were dried, and the resulting structures were observed using FE-SEM (Figure 5), as previously reported by Suzuki's group.[16-19, 36] In the case of the B100, B80M20, B50M50, and B40M60 microspheres, whose T_g values were below room temperature, it was difficult to observe individual microspheres (Figure 5), probably due to the coalescence of the microspheres when they are completely dried.[37] On the other hand, for B30M70, B20M80, and M100 microspheres, cracks were observed in the microsphere aggregates formed at the edges of the droplets (Figure 5). In general, cracks in latex films negatively affect their mechanical properties.[32] In this study, these cracks were believed to inhibit latex film formation (Figure 3, Figure 4) and lead to weak mechanical properties in the films (*vide infra*).

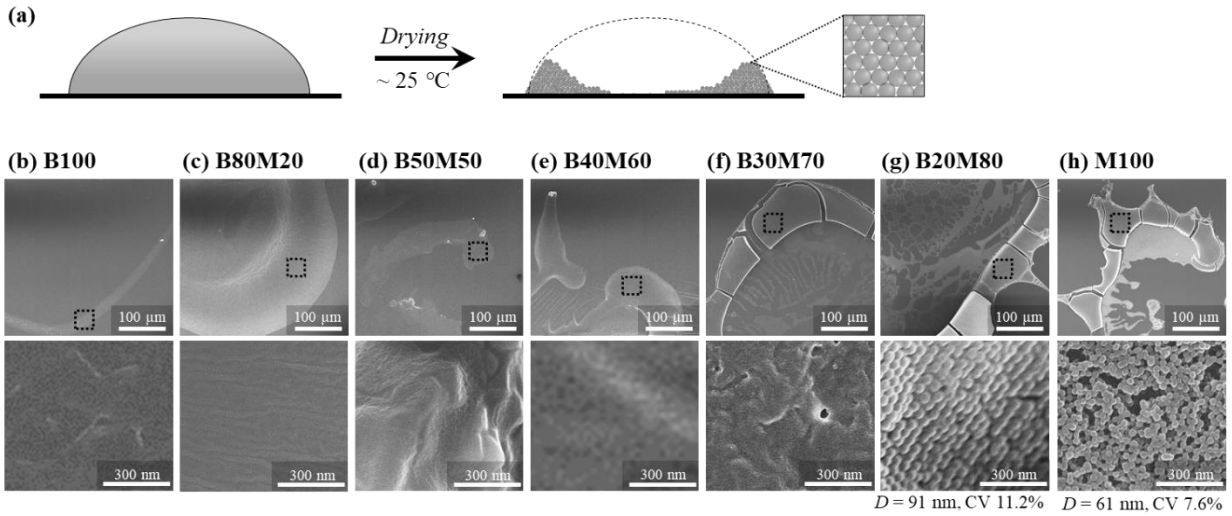

Figure 5. (a) Schematic illustration of the drying phenomenon of B*X*M*Y* microsphere droplets. (b)-(h) FE-SEM images showing the post-drying structure of droplets of poly(BA-*co*-MMA).

Next, the surfaces of latex films prepared by injecting the B40M60 dispersion into a mold and drying it at different FFTs were observed using AFM (Figure 6) in order to discuss the effect of the FFT on the nanostructure of the film surface. The microsphere morphology could still be observed in the film dried at 10 °C and 25 °C, unlike in the latex films prepared at temperatures greater than the T_g (24 °C), i.e., 40 °C (Figure 6). The author hypothesized that the spherical

morphology of the microspheres was retained not only on the film surface, but also within the film. These results confirm that the FFT affected the deformability of the microspheres, and thus the nanostructure of the latex films.

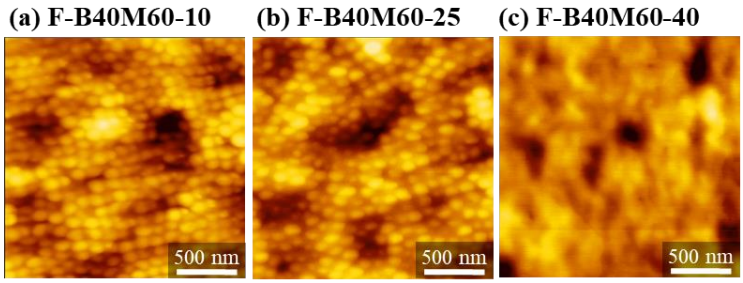

Figure 6. AFM image of the surface of (a) F-B40M60-10, (b) F-B40M60-25, and (c) F-B40M60-40 at room temperature.

Subsequently, the latex films were quantitatively evaluated in terms of the interpenetration between the microspheres, i.e., the characteristic interfacial thickness (t_{inter}) was calculated based on the SAXS data using Porod's law. [33] Figure 7 (a) shows the SAXS profiles of the latex films F-B40M60-*Z* (*Z* = 10, 25, and 40), which were prepared by drying B40M60 at 10 °C, 25 °C, and 40 °C. The SAXS intensity peaks were broad and did not show significant change at different drying temperatures. Furthermore, the sharpness of the peak depends on the polydispersity of the microspheres and their arrangement, making it thus difficult to discuss its significance. In a previous study, these peaks were attributed to the ordered structure of microspheres in the latex film, with the Bragg peaks originating from face-centered cubic (fcc) colloidal crystals.[26] The Bragg peaks, e.g., q111, also shifted to higher scattering vector (q) values upon annealing due to the decrease in the center-to-center distance between the B40M60 microspheres (Figure 8). The t_{inter} value, which is an indicator of the degree of interdiffusion of polymer chains between neighboring microspheres, was calculated. The calculated t_{inter} values of the unannealed films decreased in the order F-B40M60-40 (3.4 nm) > F-B40M60-25 (3.3 nm) > F-B40M60-10 (2.9 nm) (Table 2; annealing time: 0 h). Then, the author investigated the effect of annealing on the t_{inter} values of the latex films. Figure 7 (b) shows the t_{inter} values of F-B40M60-*Z* as a function of the annealing time at 70 °C. For all the films, the calculated t_{inter} value initially increased with increasing annealing time before it reached an equilibrium value (Figure 7 (b); F-B40M60-10: ~3.2 nm, F-B40M60-25: ~3.6 nm, F-B40M60-40: ~3.6 nm), indicating that the temperature

dependence of the polymer chain diffusivity is also inherited by the polymer chain diffusivity at the interface of the microsphere surface. [33]

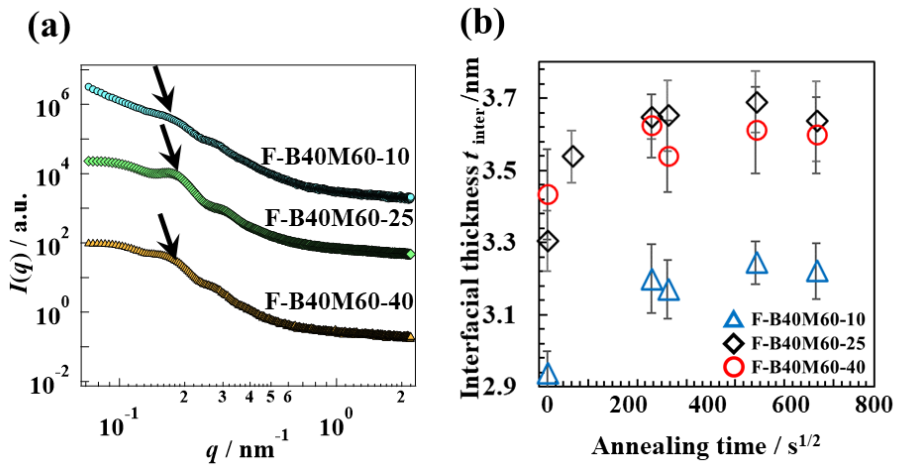

Figure 7. (a) SAXS intensities of F-B40M60-10, F-B40M60-25, and F-B40M60-40. The peaks indicated by arrows correspond to $q111$. (b) Interfacial thickness (t_{inter}) of F-B40M60-10 (triangles), F-B40M60-25 (diamonds), and F-B40M60-40 (circles) as a function of the annealing time. The t_{inter} value of F-B40M60-25 was reproduced with permission from reference 33. Copyright (2020) American Chemical Society.

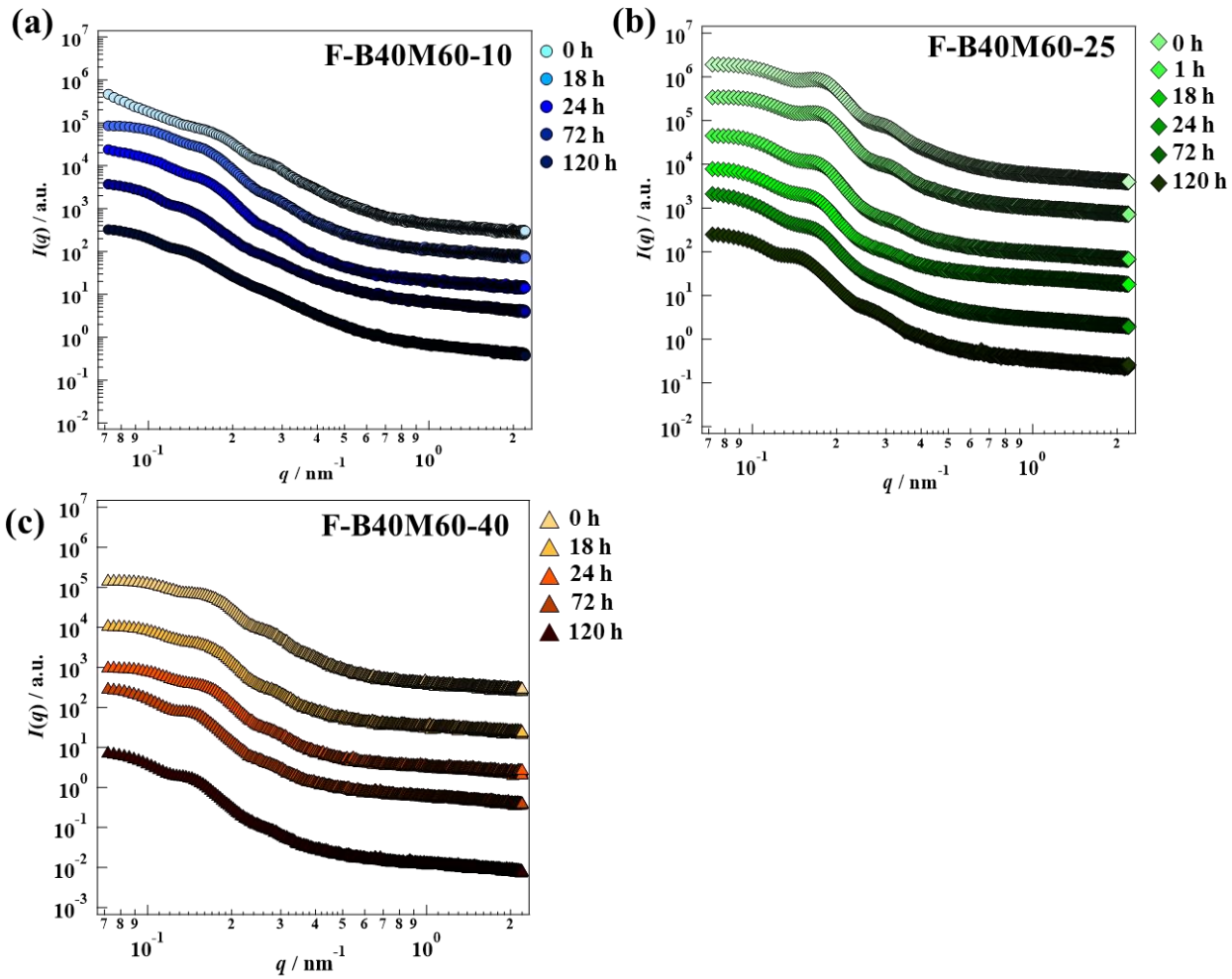

Figure 8. SAXS intensities of latex films of **(a) F-B40M60-10** (FTT < T_g), **(b) F-B40M60-25** (FTT > T_g), and **(c) F-B40M60-40** (FTT > T_g).

Table 2. Characterization of **F-B40M60-10, F-B40M60-25**, and **F-B40M60-40** latex films.

Sample	FFT (°C)	Annealing time (h)	Interfacial thickness (nm)
F-B40M60-10	10	0	2.94
		18	3.20
		24	3.17
		72	3.24
		120	3.22
F-B40M60-25	25	0	3.3
		18	3.6
		24	3.7
		72	3.7
		120	3.6
F-B40M60-40	40	0	3.43
		18	3.62
		24	3.54
		72	3.61
		120	3.60

Data for **F-B40M60-25** were reproduced with permission from ref 1. Copyright (2020) American Chemical Society.

Mechanical Properties of Latex Films

After evaluating the structures of the latex films of poly(BA-*co*-MMA) as discussed above, the author investigated the mechanical properties or toughness of the self-standing latex films. First, the latex films were evaluated by hand-stretching. The latex films of B50M50 (FFT: 4 °C) and B40M60 (FFT: 25 °C) could be stretched by hand. In contrast, the latex films of B30M70 (FFT: 40 °C) and B20M80 (FFT: 70 °C) were hard and brittle and broke immediately. Next, mechanical properties of the latex films were evaluated by tensile tests. The stress of the B50M50 latex film did not rise, and necking was observed (Figure 9 (a)). The Young's modulus, which is an indicator of the stiffness of a solid material, was obtained from the stress–strain curves for a series of latex films (Figure 9, Table 3). The Young's moduli of the B40M60 latex films were lower than those of B20M80 (105 MPa at FFT 70 °C) and B30M70 (86 MPa at FFT 40 °C, 106 MPa at FFT 70 °C), indicating that the degree of microsphere deformation decreases with increasing MMA content in the microspheres. These data clearly show that slight differences in the BA:MMA ratio of the microspheres greatly affect the mechanical properties of the latex films. In the case of the B40M60 latex films, the Young's modulus increased with the FFT (3.1, 3.1, 8.2, and 13.1 MPa at FFT 10,

25, 40, and 70 °C, respectively; Table 3), indicating that the FFT did affect the mechanical properties of the latex films. It is widely accepted that non-uniform structures such as cracks or voids, the crucial factors affecting mechanical properties of latex films, disappeared with increasing FFT due to the softening of the microspheres,[38] which would affect the result of the present study.

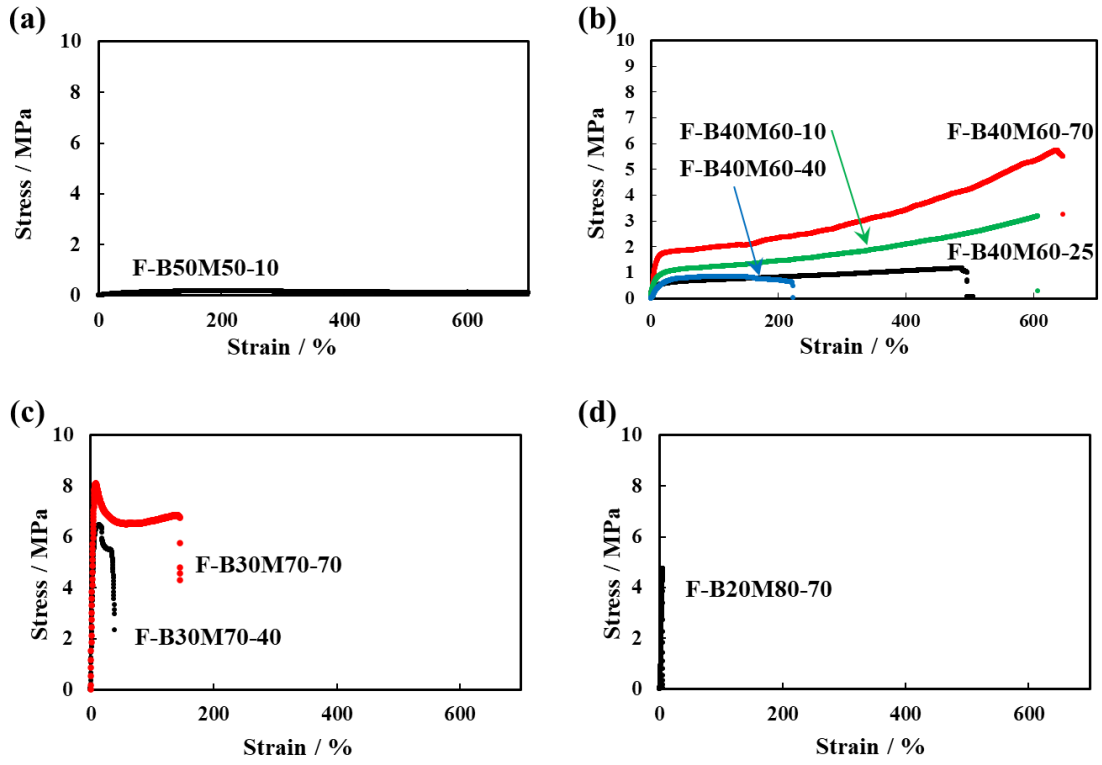

Figure 9. Stress–strain curves for latex films of **(a) F-B50M50-10**, **(b) F-B40M60-10**, **25**, **40**, **70** **(c) F-B30M70-40**, **70**, and **(d) F-B20M80-70** microspheres.

Table 3. Characterization of the **B*X*M*Y*** latex films.

Sample	FFT (℃)	Young's modulus (MPa)	Fracture strain (%)	Fracture stress (MPa)	Fracture energy (MJ/m^3)
B20M80	70	1.05	5.7	4.7	0.14
B30M70	40	0.86	34	5.4	2.1
	70	1.06	144	6.8	10.3
B40M60	10	0.031	222	0.6	0.51
	25	0.031	489	1.2	4.0
	40	0.082	606	3.1	11.5
	70	0.131	640	5.6	21.4

Figure 10 (a)(b) show the stress–strain curves of F-B40M60-10 and F-B40M60-40 films prepared using different annealing times. The effect of the annealing time on the mechanical properties was evaluated by calculating the fracture energy (Figure 10 (c)). The annealing of latex films has previously been reported to increase their fracture energy, making the films mechanically tougher. [32, 35] As expected, the fracture energy of these latex films increased with increasing annealing time; this effect was stronger for F-B40M60-40 than for F-B40M60-10 and F-B40M60-25 (Figure 10 (c)). The fracture energies reached equilibrium values after long annealing times (Figure 10 (c): F-B40M60-10: ~13.4 MJ/m^3, F-B40M60-25: ~15.0 MJ/m^3, F-B40M60-40: ~26.1 MJ/m^3). At this point, the author believes that the neighboring microspheres in latex films were sufficiently coalesced and that the surface polymer chains were mixed after annealing the films above the T_g of the microspheres. In this study, the coalescence of the microspheres was found to be strongly promoted during drying of the dispersion when the latex films were prepared by evaporation at 40 °C, which is a crucial factor in producing tough latex films. Film formation at 40 °C greatly enhanced the interdiffusion between the microspheres, as can be seen in Figure 7 (b). The film formed at 25 °C (F-B40M60-25) showed a similar tendency (Figure 7 (b)) to that formed at 40 °C (F-B40M60-40); however, the microspheres in F-B40M60-25 remained spherical (Figure 6 (b)), which should affect its fracture energy (Figure 10 (c)). In conclusion, breakage at the interface of neighboring microspheres is inhibited by both increasing the contact area between the microsphere interfaces and increasing interfacial thickness. For these reasons, the fracture energy of the fully annealed F-B40M60-40 was higher than that of F-B40M60-10 and F-B40M60-25.

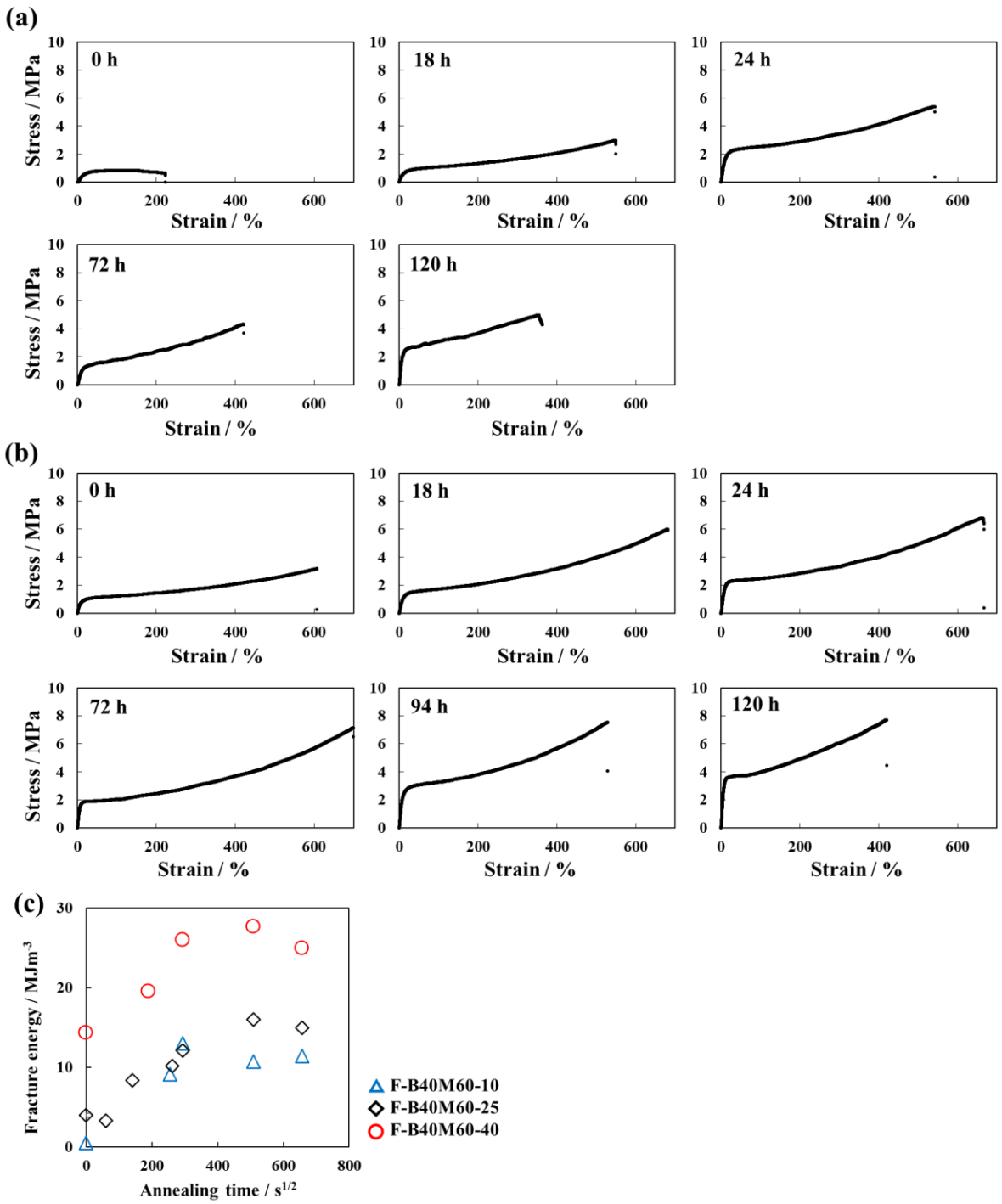

Figure 10. Stress–strain curves of (a) F-B40M60-10 (FFT < T_g) and (b) F-B40M60-40 (FFT > T_g) for different annealing times. (c) Fracture energy values as a function of the square root of the annealing time for F-B40M60-10 (triangles), F-B40M60-25 (diamonds), and F-B40M60-40 (circles).

2.4. Conclusions

The author have investigated the relationship between the (nano)structures and mechanical properties of the latex films formed at different film-formation temperatures (FFT) using a series of poly(BA-*co*-MMA) microspheres above and below the glass-transition temperature (T_g) of the microspheres. The T_g of the microspheres could be tuned simply by changing the BA/MMA monomer ratio during the mini-emulsion polymerization. A series of films were prepared by drying dispersions of the various poly(BA-*co*-MMA) microspheres at different FFTs. An analysis of the resulting films revealed that the formation of self-standing latex films depends on the deformability of the microspheres (FFT > T_g). Specifically, self-standing and stretchable latex films are obtained for a narrow composition window, i.e., microspheres prepared using a **B40M60**. The toughness or fracture energy of the films was strongly correlated to the interfacial diffusion between microspheres, which increases when the films are prepared at higher temperatures and after annealing. Most notably, the FFT is crucial to obtaining tough latex films, since films obtained using a suitably high FFT are highly coalescent, and their surface polymer chains are highly interdiffused after annealing.

2.5. References

[1] Routh, A. F. Drying of Thin Colloidal Films. *Rep. Prog. Phys.,* 76, 046603, **2013**.

[2] Schulz, M. Keddie, J. L. A Critical and Quantitative Review of the Stratification of Particles During the Drying of Colloidal Films. *Soft Matter,* 14, 6181−6197, **2018**.

[3] Jiang, S. Van Dyk, A. Maurice, A. Bohling, J. Fasano, D. Brownell, S. Design Colloidal Particle Morphology and Self-Assembly for Coating Applications. *Chem. Soc. Rev.,* 46, 3792–3807, **2017**.

[4] Limousin, E. Ballard, N. Asua, J. M. Soft Core–Hard Shell Latex Particles for Mechanically Strong VOC-Free Polymer Films. *J. Appl. Polym. Sci.,* 136, 47608, **2019**.

[5] Lambourne, R. and Strivens, T. A. Paint and Surface Coatings. *Woodhead Publishing Ltd.*, **1999**.

[6] Liu, M. Mao, X. Zhu, H. Lin, A. Wang, D. Water and Corrosion Resistance of Epoxy–Acrylic–Amine Waterborne Coatings: Effects of Resin Molecular Weight, Polar Group and Hydrophobic Segment. *Corros. Sci.,* 75, 106–113, **2013**.

[7] Gurney, R. S. Dupin, D. Nunes, J. S. Ouzineb, K. Siband, E. Asua, J. M. Armes, S. P. Keddie, J. L. Switching Off the Tackiness of a Nanocomposite Adhesive in 30 s via Infrared Sintering. *ACS Appl. Mater. Interfaces*, 4, 5442−5452, **2012**.
[8] Calvo, M. E. Míguez, H. Flexible, Adhesive, and Biocompatible Bragg Mirrors Based on Polydimethylsiloxane Infiltrated Nanoparticle Multilayers. *Chem. Mater.*, 22, 3909–3915, **2010**.
[9] Sababi, M. Kettle, J. Rautkoski, H. Claesson, P. M. Thormann, E. Structural and Nanomechanical Properties of Paperboard Coatings Studied by Peak Force Tapping Atomic Force Microscopy. *ACS Appl. Mater. Interfaces*, 4, 5534−5541, **2012**.
[10] Lee, J.-H. Lee, H. L. Characterization of the Paper Coating Structure Using Focused Ion Beam and Field-Emission Scanning Electron Microscopy. 2. Structural Variation Depending on the Glass Transition Temperature of an S/B Latex. *Ind. Eng. Chem. Res.*, 57, 16718–16726, **2018**.
[11] Viel, B. Ruhl, T. Hellmann, G. P. Reversible Deformation of Opal Elastomers. *Chem. Mater.*, 19, 5673–5679, **2007**.
[12] Schäfer, C. G. Smolin, D. A. Hellmann, G. P. Gallei, M. Fully Reversible Shape Transition of Soft Spheres in Elastomeric Polymer Opal Films. *Langmuir*, 29, 11275–11283, **2013**.
[13] Ito, T. Katsura, C. Sugimoto, H. Nakanishi, E. Inomata, K. Strain-Responsive Structural Colored Elastomers by Fixing Colloidal Crystal Assembly. *Langmuir*, 29, 13951–13957, **2013**.
[14] Kureha, T. Hiroshige, S. Matsui, S. Suzuki, D. Water-Immiscible Bioinert Coatings and Film Formation from Aqueous Dispersions of Poly(2-methoxyethyl acrylate) Microspheres. *Colloids Surf., B*, 155, 166–172, **2017**.
[15] Marchetti, P. Mechelhoff, M. Livingston, A. G. Tunable-Porosity Membranes from Discrete Nanoparticles. *Sci. Rep.*, 5, 17353, **2015**.
[16] Horigome, K. Suzuki, D. Drying Mechanism of Poly(*N*-isopropylacrylamide) Microgel Dispersions. *Langmuir*, 28, 12962-12970, **2012**.
[17] Suzuki, D. Horigome, K. Assembly of Oppositely Charged Microgels at the Air/Water Interface. *J. Phys. Chem. B*, 117, 9073-9082, **2013**.
[18] Takizawa, M. Sazuka, Y. Horigome, K. Sakurai, Y. Matsui, S. Minato, H. Kureha, T. Suzuki, D. Self-organization of Soft Hydrogel Microspheres during the Evaporation of Aqueous Droplets. *Langmuir*, 34, 4515-4525, **2018**.

[19] Minato, H. Takizawa, M. Hiroshige, S. Suzuki, D. Effect of Charge Groups Immobilized in Hydrogel Microspheres during the Evaporation of Aqueous Sessile Droplets. *Langmuir*, 35, 10412-10423, **2019**.
[20] Taylor, J. W. Winnik, M. A. Functional Latex and Thermoset Latex Films. *J. Coat. Technol. Res.*, 1, 163–190, **2004**.
[21] Lohmeijer, B. Balk, R. Baumstark, R. Preferred Partitioning: The Influence of Coalescents on the Build-up of Mechanical Properties in Acrylic Core–Shell Particles (I). *J. Coat. Technol. Res.*, 9, 399–409, **2012**.
[22] Gauthier, C. Sindt, O. Vigier, G. Guyot, A. Schoonbrood, H. A. S. Unzue, M. Asua, J. M. Reactive Surfactants in Heterophase Polymerization. XVII. Influence of the Surfactant on the Mechanical Properties and Hydration of the Films. *J. Appl. Polym. Sci.*, 84, 1686–1700, **2002**.
[23] Asua, J. M. Schoonbrood, H. A. S. Reactive Surfactants in Heterophase Polymerization. *Acta Polym.*, 49, 671–686, **1998**.
[24] Aramendia, E. Mallégol, J. Jeynes, C. Barandiaran, M. J. Keddie, J. L. Asua, J. M. Distribution of Surfactants near Acrylic Latex Film Surfaces: A Comparison of Conventional and Reactive Surfactants (Surfmers). *Langmuir*, 19, 3212–3221, **2003**.
[25] Eckersley, S. T. Helmer, B. J. Mechanistic Considerations of Particle Size Effects on Film Properties of Hard/Soft Latex Blends. *J. Coat. Technol*, 69, 97–107, **1997**.
[26] Tzitzinou, A.; Keddie, J. L. Geurts, J. M. Peters, A. C. I. A. Satguru, R. Film Formation of Latex Blends with Bimodal Particle Size Distributions: Consideration of Particle Deformability and Continuity of the Dispersed Phase. *Macromolecules,* 33, 2695–2708, **2000**.
[27] Geurts, J. Bouman, J. Overbeek, A. New Waterborne Acrylic Binders for Zero VOC Paints. *J. Coat. Technol. Res.*, 5, 57–63, **2008**.
[28] Liu, Y. Schroeder, W. Soleimani, M. Lau, W. Winnik, M. A. Effect of Hyperbranched Poly(butyl methacrylate) on Polymer Diffusion in Poly(butyl acrylate-*co*-methyl methacrylate) Latex Films. *Macromolecules*, 43, 6438–6449, **2010**.
[29] Zohrehvand, S. te Nijenhuis, K. Film Formation from Monodisperse Acrylic Latices, Part 4: The Role of Coalescing Agents in the Film Formation Process. *Colloid Polym. Sci.*, 283, 1305–1312, **2005**.

[30] Divry, V. Gromer, A. Nassar, M. Lambour, C. Collin, D. Holl, Y. Drying Mechanisms in Plasticized Latex Films: Role of Horizontal Drying Fronts. *J. Phys. Chem. B*, 120, 6791–6802, **2016**.
[31] Hiroshige, S. Kureha, T. Aoki, D. Sawada, J. Aoki, D. Takata, T. Suzuki, D. Formation of Tough Films by Evaporation of Water from Dispersions of Elastomer Microspheres Crosslinked with Rotaxane Supramolecules. *Chem. – Eur. J.*, 23, 8405–8408, **2017**.
[32] Hiroshige, S. Sawada, J. Aoki, D. Takata, T. Suzuki, D. Investigation of Mechanical Properties of Latex Films Prepared from Poly (Butyl Acrylate-*co*-Methyl Methacrylate) Microspheres Crosslinked with Rotaxane. *Nihon Reoroji Gakkaishi*, 47, 051–054, **2019**.
[33] Kureha, T. Hiroshige, S. Suzuki, D. Sawada, J. Aoki, D. Takata, T. Shibayama, M. Quantification for the Mixing of Polymers on Microspheres in Waterborne Latex Films. *Langmuir*, 36, 4855–4862, **2020**.
[34] Antonietti, M. Landfester, K. Polyreactions in Miniemulsions. *Prog. Polym. Sci.*, 27, 689–757, **2002**.
[35] Zosel, A. Ley, G. Influence of Cross-Linking on Structure, Mechanical Properties, and Strength of Latex Films. *Macromolecules*, 26, 2222–2227, **1993**.
[36] Honda, K. Sazuka, Y. Iizuka, K. Matsui, S. Uchihashi, T. Kureha, T. Shibayama, M. Watanabe, T. Suzuki, D. Hydrogel Microellipsoids that Form Robust String-like Assemblies at the Air/Water Interface, *Angew. Chem. Int. Ed.*, 58, 7294-7298, **2019**.
[37] Matsui, S. Kureha, T. Hiroshige, S. Shibata, M. Uchihashi, T. Suzuki, D. Fast Adsorption of Soft Hydrogel Microspheres on Solid Surfaces in Aqueous Solution. *Angew. Chem. Int. Ed.*, 56, 12146-12149, **2017**.
[38] van der Kooij, H. M. de Kool, M. van der Gucht, Sprakel, J. Coalescence, Cracking, and Crack Healing in Drying Dispersion Droplets. *Langmuir*, 31, 4419–4428, **2015**.

3. Chapter II

" Formation of Tough Films by Evaporation of Water from Dispersions of Elastomer Microspheres Crosslinked with Rotaxane Supramolecules"

*Part of this work was published in " Seina Hiroshige, Takuma Kureha, Daichi Aoki, Jun Sawada, Daisuke Aoki, Toshikazu Takata, Daisuke Suzuki *Chemistry-A Europrean Journal* **2017**, *23*, 8405 –8408, DOI: https://doi.org/10.1002/chem.201702077" Reprinted with permission from Copyright (2017) Wiley-VCH.

*Part of this work was published in " Seina Hiroshige, Jun Sawada, Daisuke Aoki, Toshikazu Takata, Daisuke Suzuki, *Nihon Reoroji Gakkaishi,* **2019**, *47*, 227-231, DOI: 10.1678/rheology.47.51" Reprinted with permission from Copyright (2019) The Society of Rheology, Japan.

3.1. Introduction

Downsizing polymer materials to the colloidal scale can lead to stable dispersions of polymer microspheres that exhibit distinctly different behavior from the corresponding bulk materials. Hence, their use in unconventional applications such as drug-delivery vehicles that aim to control the point of drug delivery in the human body becomes feasible.[1] In reverse, the corresponding bulk materials can be obtained upon evaporating the solvent from dispersions of colloidal microspheres. One of the most prominent advantages of colloidal dispersions is that they are injectable, which significantly simplifies the manufacturing of bulk materials. In contrast to rigid microspheres based on polystyrene or silica, soft and deformable elastomer microspheres have been used to create colorless transparent films through solvent evaporation, which can be rationalized in the context of the Routh–Russel model.[2] So far, various applications including coatings,[3] inkjet printing,[4] and adhesives[5] have been developed using this method. However, to obtain films with outstanding mechanical properties, chemical crosslinking among the microspheres is required.[6] Such crosslinking reactions are complex and require the presence of additives during the removal of the solvent from the dispersions. Because unreacted additives usually remain in the resulting bulk films, this film-formation technology cannot be used for

applications that do not tolerate impurities, for example, biomaterials that attach to the human body. In contrast to colloidal microspheres, bulk materials of rotaxane-crosslinked polymer networks exhibit unique properties that are not observed in conventional chemically crosslinked polymer networks.[7] Specifically, it is possible to obtain mechanically tough bulk elastomers/hydrogels by crosslinking polymers with rotaxanes. However, to the best of my knowledge, such networks with flexible crosslinks have not yet been applied to colloidal microspheres. In the present study, the author introduce for the first time such flexibly crosslinked structures into colloidal polymer microspheres (Scheme 1A) and investigate the properties of the resulting bulk elastomer films formed upon evaporating water from microsphere dispersions. To my surprise, the resulting films are mechanically tough, even though post-polymerization crosslinking reactions between the microspheres were not performed.

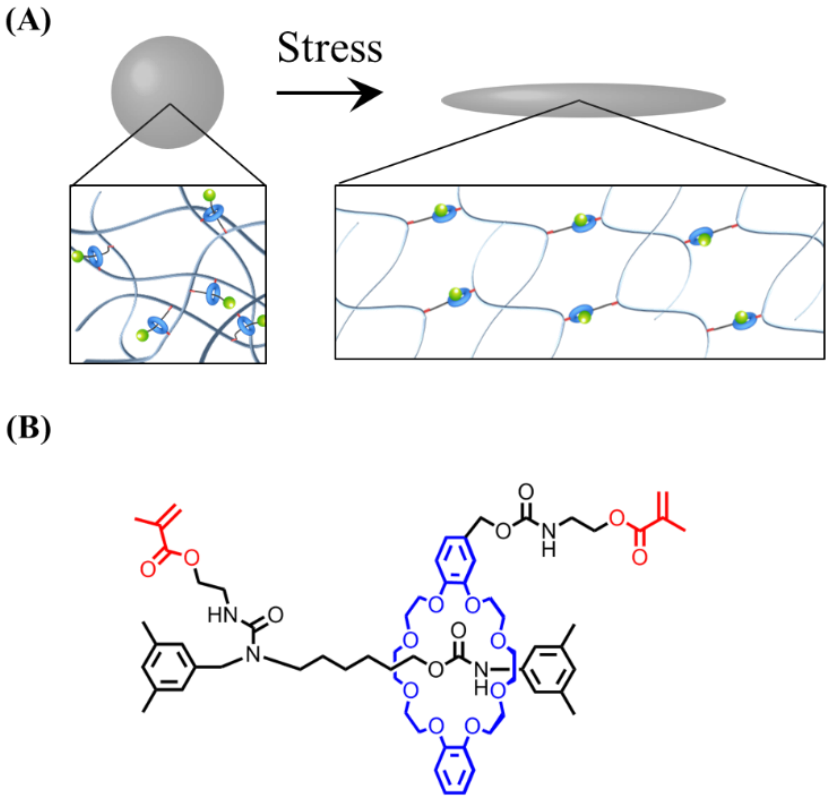

Scheme 1. (A) Schematic illustration of rotaxane-crosslinked elastomer microspheres. (B) Chemical structure of the rotaxane crosslinker (**RC**) used in this study.

3.2. Experimental Section

1. Materials

Methyl methacrylate (MMA, 98%), *n*-butyl acrylate (BA, 98%), divinylbenzene (DVB, 93%), potassium peroxodisulfate (KPS, 95%), *n*-hexadecane (HD, 97%), and *N,N*-dimethylformamide (DMF, 99%) were purchased from Wako Pure Chemical Industries (Japan) and used as received. Sodium dodecyl benzene sulfonate (DBS, 95%) and 1,6-hexanediol dimethacrylate (HDD, 98%) were purchased from Tokyo Chemical Industry Co., Ltd. (Japan) and used as received. Water for all reactions, including the preparation of solutions and the purification of polymers, was distilled and ion-exchanged (EYELA, SA-2100E1).

2. Synthesis and characterization of the [2]rotaxane cross-linker (RC).

The details of the synthesis and characterization of RC are described elsewhere.[1]

3. Synthesis of poly(BA-*co*-MMA) microspheres

Elastomer microspheres were prepared by a miniemulsion polymerization technique, using the water-soluble anionic initiator KPS. The initial total monomer concentration was held constant at 1.6 M. An oil mixture of the monomer (BA and/or MMA; *cf.* Tables 1 and 2), crosslinker (DVB, HDD, or RC), and HD (0.46 g) were suspended in water (30 mL) containing DBS (0.1 g). The suspension was subsequently exposed to ultrasonication (3 min; 375 W) from an ultrasonic homogenizer (VC-75, SONICS). Then, the suspension was transferred into a 50 mL four-necked round-bottom flask equipped with a mechanical stirrer, condenser, and nitrogen gas inlet. The solution was heated to 70 °C under a stream of nitrogen and constant stirring (200 rpm). The solution was allowed to stabilize over a period of at least 30 min before the free-radical polymerization was initiated by adding KPS (0.1 g) in water (6 mL). The stirred solution was allowed to react for a period of 4 h, before being allowed to cool to room temperature. The elastomer microspheres were purified twice by centrifugation–redispersion with water (RCF = 20000 g; 60 min), followed by dialysis for a week, whereby the water was changed daily.

4. Characterization of the elastomer microspheres

The hydrodynamic diameter of the elastomer microspheres was determined by dynamic light scattering (DLS, Malvern Instruments Ltd., Zetasizer NanoS). Data were averaged over three measurements with a 30 s acquisition time using the intensity autocorrelation. DLS experiments were conducted with an elastomer microsphere concentration of 0.001 wt%. The electrophoretic mobility was measured using a Zetasizer Nano ZS (Malvern Instruments). The optical transmittance of the films was measured on a UV−vis spectrophotometer (JASCO, V-630iRM) using pMMA disposable cells (AS ONE, 2-5719-01). Films were immobilized on the wall of the cell at a distance of 10 mm to the bottom. The measurement wavelength was 600 nm. Microspheres were used at a concentration of ~0.0002 wt%, and the ionic strength was adjusted to 1 mM with a NaCl solution. Before the measurement, the sample was allowed to equilibrate for 10 min at 25 °C. The electrophoretic mobility results represent the average of three measurements. The elastomer microspheres were analyzed by applying the Smoluchowski equation to the electrophoretic mobility. Individual microspheres were examined by atomic force microscopy (AFM, SPM-9500J3, Corporation). For the sample preparation, a microsphere dispersion (~0.008 wt%) was deposited onto a glass substrate and dried at room temperature. Tensile tests (tensilonRTC1250A, A&D Company) were performed at 25 °C using a graph equipped with a 50 N load cell at an elongation rate of 10 mm/min. The microsphere conversion was measured using a dry weight method. The dispersion of the elastomer microspheres, followed by drying at 70 °C, was calculated according to the following equation:

$$\text{conversion (\%)} = \frac{w_2}{w_1} \times \frac{M_1}{M_2} \times 100,$$

wherein W_1 refers to the weight of the microsphere dispersion, and W_2 to the weight of the solid content (after drying at 70 °C). M_1 is the weight of the total nonvolatile components in the system, while M_2 is the weight of the microspheres for the complete conversion of monomers into polymers.

5. Synthesis of microsphere films

Films were generated by depositing an elastomer microsphere dispersion (8.0 wt%, 300 μL) on a silicon rubber sheet (ISO 37-4 dumbbell-shaped specimen; 12 × 2 mm^2), followed by drying at room temperature for 24 h.

3.3. Results and discussion

3.3.1. Adsorption behavior of halogen compounds on pMEA microspheres

To obtain colloidal microspheres with flexible crosslinkers, a rotaxane crosslinker (**RC**) based on a [2]rotaxane, consisting of a crown ether wheel and an axle with one vinyl group per component, was prepared according to a previously reported method (Scheme 1B).[7g] The author selected miniemulsion polymerization[8], where an oil monomer droplet will be polymerized to be a polymer microsphere, to trap the **RC** within the microspheres sufficiently because the **RC** is hardly dissolved in water, but that can be dissolved in organic solvents or oil-monomers. Indeed, conventional emulsion polymerization could not be applied to synthesize the colloidal microspheres crosslinked with the **RC** due to their high water-immiscible property (Figure 1).

Figure 1. (A) Photograph of the reaction vessel after a conventional emulsion polymerization of BA (39.9 mol%) and MMA (59.9 mol%) in the presence of **RC** (0.2 mol%). Almost all the **RC** reagent (brown solid) was deposited in the flask, which suggests that the resulting microspheres contain very little **RC**. For the formation of poly(BA-*co*-MMA) microsphere dispersions, a mixture of BA (1.3 g, 39.9 mol%), MMA (1.5 g, 59.9 mol%), and **RC** (0.06 g, 0.2 mol%) in 200 mL of water was poured into a 200 mL four-necked, round-bottom flask equipped with a condenser and a mechanical stirrer. The mixture was heated to 70 °C while being stirred at 300 rpm. The polymerization was initiated by addition of KPS (0.0271 g) in water (5 mL), and allowed to proceed for 24 h. (B) Photograph of **RC**.

Butyl acrylate (BA) and methyl methacrylate (MMA) were chosen as monomers, which resulted in the formation of colorless transparent films after of evaporation of the solvent from the thus obtained dispersions. As demonstrated in a previous report,[9] the copolymerization of MMA was necessary to obtain self-standing films after evaporation of the solvent, as bulk films of microspheres composed of only poly-BA or poly-MMA were not self-standing. The evaporation of the solvent from a dispersion containing microspheres of a copolymer of ~40 mol% BA and ~60 mol% MMA afforded the best results (Table 1 and Figure 2). Prior to any characterization of the microspheres (*vide infra*), impurities such as the surfactant sodium dodecyl benzene sulfonate were removed via dialysis and centrifugation.

Table 1. Composition, hydrodynamic diameters (D_h), conversion, and polydispersity indexes of several copolymer microspheres obtained from mini-emulsion polymerizations in the absence of any crosslinkers.

	Monomer		D_h	PDI	Conversion
	BA	MMA			
	[mol%]	[mol%]	[nm]		[%]
BA	100 (7.4 g)	0 (0 g)	131 ± 1.2	0.054	99
BA80-MMA20	80 (5.9 g)	20 (1.2 g)	112 ± 0.6	0.030	96
BA60-MMA40	60 (4.4 g)	40 (2.3 g)	101 ± 0.2	0.042	95
BA50-MMA50	50 (3.7 g)	50 (2.9 g)	108 ± 1.0	0.044	87
BA40-MMA60	40 (3.0 g)	60 (3.5 g)	95 ± 1.0	0.041	83
BA30-MMA70	30 (2.2 g)	70 (4.6 g)	93 ± 0.2	0.043	90
MMA	0 (0 g)	100 (5.8 g)	87 ± 0.5	0.038	75

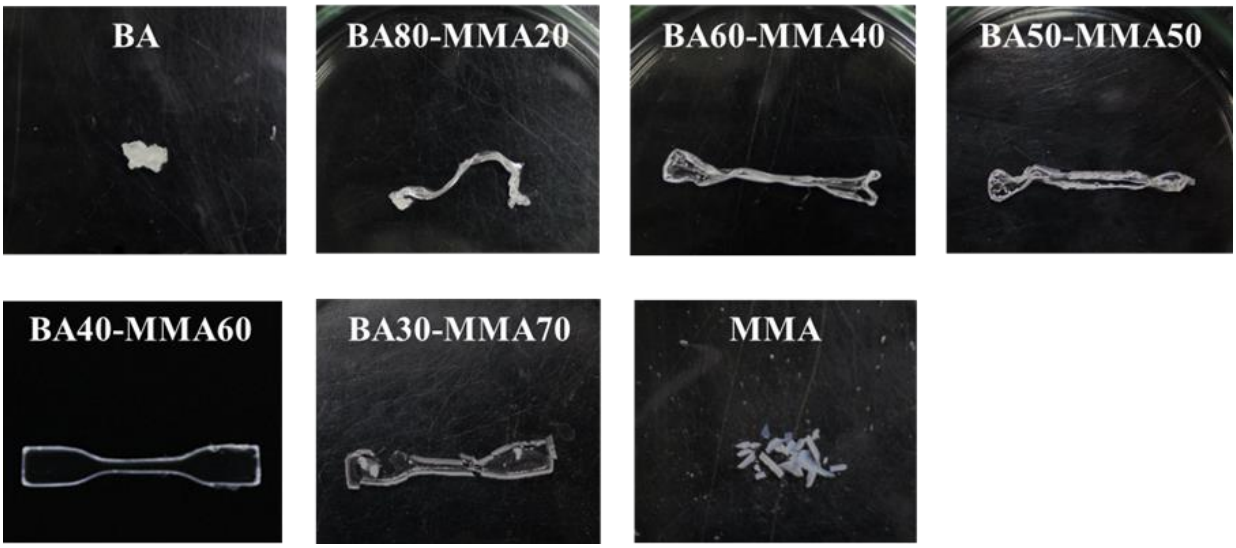

Figure 2. Photographs of films formed upon evaporating water from dispersions containing various microspheres copolymerized in the absence of **RC** (for sample codes, see Table 1). Films were obtained from depositing dispersions (8.0 wt%, 300 μL) in a mold (ISO 37-4 dumbbell-shaped specimens, 12 × 2 mm^2), followed by drying at room temperature for 24 h, before the films were removed from the mold. The results show that only copolymerizations of BA and MMA afford colorless, transparent, and self-standing films.

Figure 3A shows a representative atomic force microscopy (AFM) image of poly(BA-*co*-MMA) microspheres crosslinked with 0.05 mol% **RC** (denoted as BM-R*X*; B = ~40 mol% BA; M = ~60 mol% MMA; R = **RC**; *X* = mol% **RC**; *cf.* Table 2). From this image, the size of the microspheres (~170 nm) and their uniformity (CV = 14 %, *N* = 50) were determined. Dynamic light scattering (DLS) was used to evaluate the hydrodynamic diameter of these microspheres (D_h = ~97 nm; PDI = 0.02), which indicates that the microspheres were deformed on the glass substrate (Figure 1A). The AFM image was also used to estimate the height and uniformity of these microspheres (*h* = ~54 nm; CV = 17%, *N* = 50), which supports the aforementioned results. Other microspheres, crosslinked with the conventional chemical crosslinker divinylbenzene (DVB, 0.05~3 mol%) or different amounts of **RC** (0.03~0.5 mol%), revealed similar properties for the microspheres shown in Figure 1A, i.e., D_h ~ 100 nm and deformation on the solid substrates upon drying. These results indicate that these microspheres possess elastic properties (*cf.* Table 2 and Figure 4).

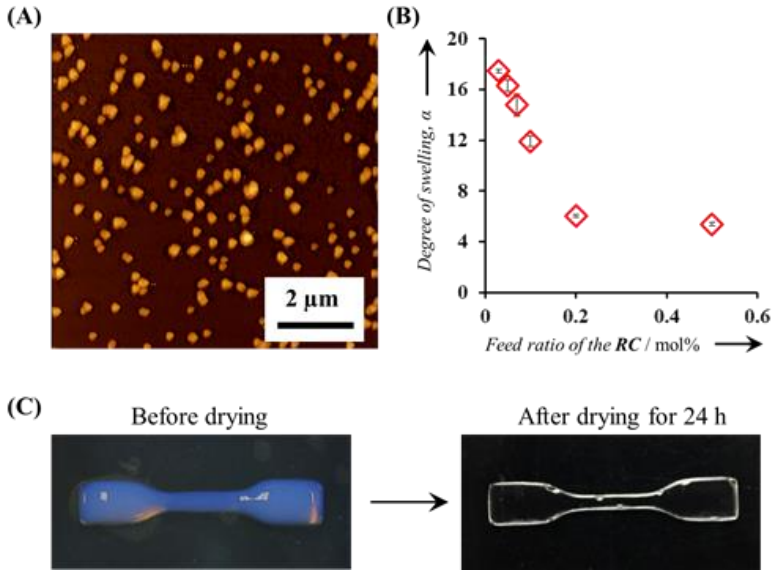

Figure 3. (A) Representative AFM image of **RC**-crosslinked microspheres BM-R0.05 (mol% BA:MMA = 40:60; **RC** = 0.05 mol%). (B) The degree of swelling, α, for **RC**-crosslinked microspheres (0.03 ~ 0.5 mol%); $\alpha = D_h^3$ (DMF) / D_h^3 (water). (C) Photographs of the film formation upon evaporating water from the microsphere dispersions at room temperature.

Table 2. Composition, hydrodynamic diameters (D_h), polydispersity indexes (PDI), zeta potentials, conversion rates, and degree of swelling for a series of copolymerized microspheres prepared by mini-emulsion polymerizations in the presence of DVB or **RC**.

	Monomer		Cross-linker		D_h	PDI	Zeta potential	Conversion	Degree of swelling,α [a]
	BA	MMA	**RC**	DVB					
	[mol%]	[mol%]	[mol%]	[mol%]	[nm]		[mV]	[%]	[%]
BM	40 (2.9 g)	60 (3.5 g)	0	0	95 ± 1.0	0.041	−46.1	83	NA
BM-D0.05	39.98 (2.9 g)	59.97 (3.5 g)	0	0.05 (0.004 g)	115 ± 1.1	0.057	−48.3	85	12.8
BM-D0.2	39.92 (2.9 g)	59.88 (3.5 g)	0	0.20 (0.015 g)	95 ± 0.2	0.036	−48.0	83	8.4
BM-D0.45	39.98 (2.9 g)	59.73 (3.5 g)	0	0.45 (0.036 g)	123 ± 0.6	0.054	−52.9	81	4.5
BM-D1.3	39.48 (2.9 g)	59.22 (3.5 g)	0	1.3 (0.10 g)	108 ± 0.8	0.036	−45.2	91	2.6
BM-D3.0	38.8 (2.9 g)	58.2 (3.5 g)	0	3.0 (0.23 g)	97 ± 0.6	0.046	−54.7	81	2.7
BM-R0.03	39.99 (2.9 g)	59.98 (3.5 g)	0.03 (0.02 g)	0	106 ± 0.8	0.038	−50.3	97	17.5
BM-R0.05	39.98 (2.9 g)	59.97 (3.5 g)	0.05 (0.034 g)	0	96 ± 1.5	0.020	−40.2	89	16.3
BM-R0.07	39.97 (2.9 g)	59.96 (3.5 g)	0.07 (0.047 g)	0	92 ±0.1	0.028	-47.4	87	14.8
BM-R0.1	39.96 (2.9 g)	59.94 (3.5 g)	0.1 (0.068 g)	0	101 ± 0.2	0.043	−43.2	94	11.9
BM-R0.2	39.92 (2.9 g)	59.88 (3.5 g)	0.2 (0.13 g)	0	104 ± 0.6	0.063	−58.3	90	6.0
BM-R0.5	39.8 (2.9 g)	59.7 (3.5 g)	0.5 (0.34 g)	0	104 ± 0.5	0.052	−43.1	92	5.4

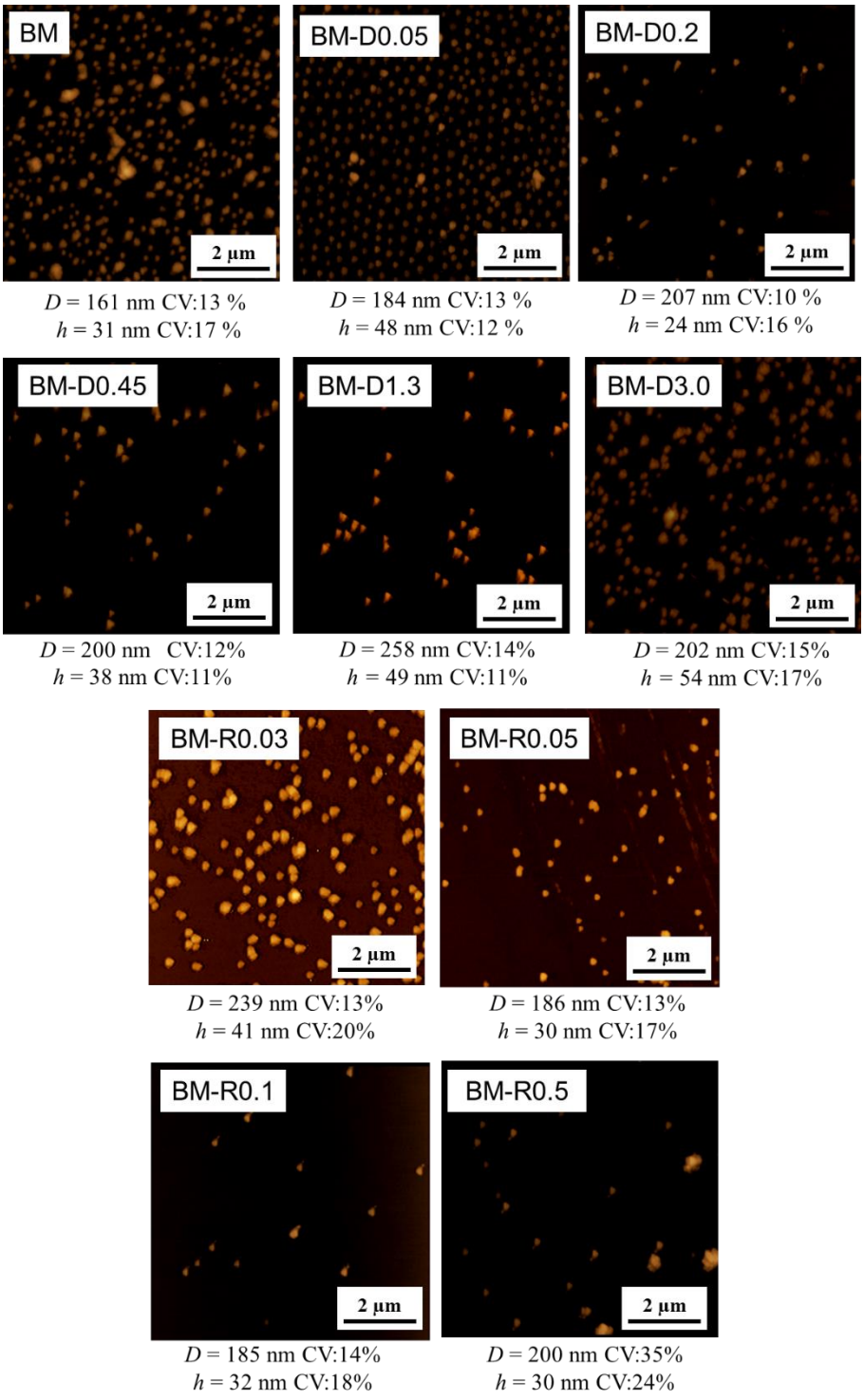

Figure 4. AFM images of DVB- or **RC**-crosslinked elastomer microspheres. The BA:MMA monomer ratio kept constant at 40:60 (mol%) during the mini-emulsion polymerization (for sample codes, see Table 2). The size (*D*) and height (*h*) of each set of microspheres is given below the individual images (*N* = 50).

Subsequently, a swelling test was carried out in order to verify whether **RC** was successfully introduced in the microspheres. Figure 1B shows the degree of swelling, α, which is defined as the ratio between D_h^3 (DMF) and D_h^3 (water); the microspheres show high and low solubility in DMF and water, respectively). Microspheres obtained from mini-emulsion polymerizations in the absence of any crosslinkers dissolved completely in DMF. In contrast, microspheres prepared in the presence of **RC** (0.03~0.5 mol%) swelled, but did not dissolve completely in DMF, suggesting that **RC** was introduced in the microspheres during the polymerization. Increasing the amount of **RC** during the polymerization led to decreased α values, which supports the successful incorporation of **RC** as crosslinkers (Figure 1B). DVB-crosslinked microspheres exhibited similar behavior, i.e., increasing the amount of DVB during the polymerization resulted in lower degrees of swelling of the microspheres (*cf.* Figure 5), indicating that mini-emulsion polymerization effectively introduces water-immiscible crosslinkers into the resulting microspheres. Dispersions of these microspheres were subsequently used to generate thin films upon evaporating water at room temperature. Irrespective of the relative amount of **RC**, flexible thin films were obtained from all **RC**-crosslinked microspheres (Figures 3C and 6).

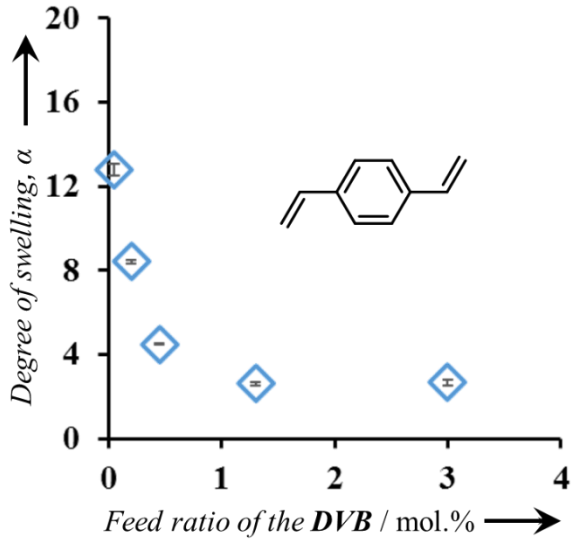

Figure 5. The degree of swelling, α, for DVB-crosslinked microspheres (0.05~3.0 mol%); $\alpha = D_h^3$ (DMF) / D_h^3 (H_2O).

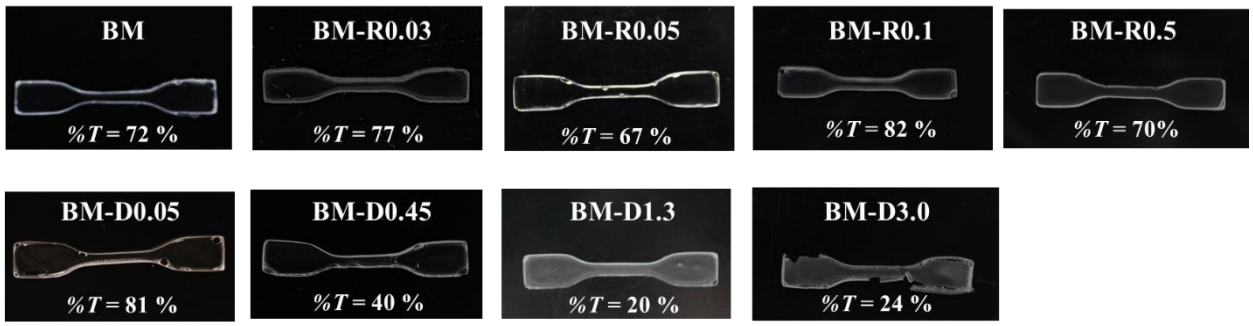

Figure 6. Photographs of films examined by tensile tests. All films, except BM-D1.3 and BM-D3.0, were flexible, and the transmittance of the films was measured by UV-vis spectroscopy at 600 nm.

Then, the author investigated the toughness of the thin films with tensile tests. Initially, the effect of the amount of **RC** in each microsphere on the toughness of the resulting films was examined (Figure 7A), which revealed a higher fracture strain for the BM-R0.05 film (885%) relative to a film of BM-R0.03 (572%). However, the fracture strain and stress values for films of BM-R0.1 (360%; 2.7 MPa) and BM-R0.5 (350%; 3.0 MPa) are substantially lower than those of BM-R0.05 (885%; 4.5 MPa). This may be due to the increasing number of crosslinking points in both films, which should suppress the deformation of the individual microspheres (Figure 7B). Consequently, an optimal chemical composition of the microspheres should exist that affords tough films. Subsequently, the toughness of films prepared from microspheres crosslinked with DVB or in the absence of **RC** was compared to the values shown in Figure 7B. Keeping the molar ratio of the crosslinkers (**RC** or DVB) in the microspheres constant (0.05 mol%) revealed a higher toughness for the film of **RC**-crosslinked microspheres (Figure 7A). As previously demonstrated, films obtained from microspheres crosslinked with the conventional crosslinker DVB (BM-D0.05) or in the absence of a crosslinker (BM) were brittle.[10] It should be noted that the distribution of crosslinking points in the microspheres should be different for acrylate-based crosslinker DVB and the methacrylate-based crosslinker **RC**, due to the different reactivity of the monomers. However, DVB-crosslinked microspheres should represent suitable controls, as films obtained from microspheres crosslinked with the methacrylate-based crosslinker 1,6-hexanediol dimethacrylate (HDD) are also brittle (Figure 7B). Films prepared from microspheres crosslinked with a higher amount of DVB exhibited increased strength, but decreased fracture strain.

Accordingly, the fracture energy, which is used as an indicator for toughness, should also be decreased (Figure 8).

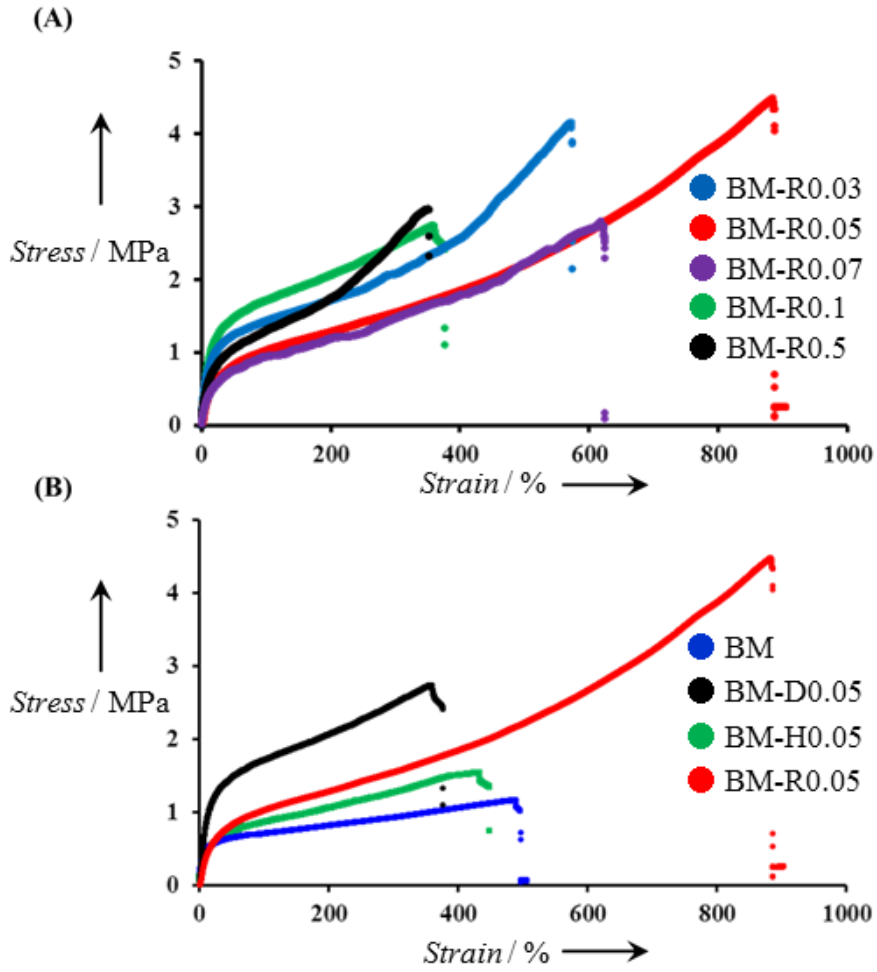

Figure 7. Stress–strain curves for films prepared from **RC**-crosslinked microspheres (BM-R*X*) (A); stress–strain curves for films prepared from microspheres without a crosslinker (blue), for films using 0.05 mol% DVB as a crosslinker (black), for films using 0.05 mol% HDD (green), or for films using 0.05 mol% **RC** (B). The film thickness was ~0.16 mm in all cases.

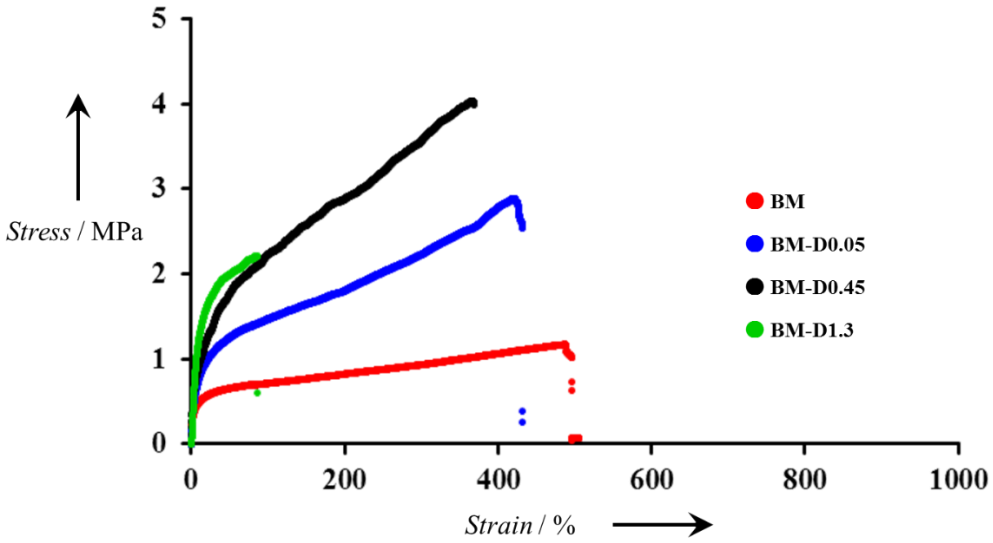

Figure 8. Stress–strain curves for films (thickness: ~0.16 mm) prepared from DVB-crosslinked microspheres (BM-D*X*).

Based on the aforementioned results in their entirety, the author would like to propose a plausible mechanism for the high toughness of the films prepared from **RC**-crosslinked microspheres (Scheme 2). It is widely accepted that the toughness of films prepared from microspheres should be attributed to the interdiffusion process, i.e., the entanglement between the polymers on each microsphere interface after removing the water.[10] The BM and BM-D films, wherein the microspheres are crosslinked only physically, are therefore brittle, as the chain entanglement between the microspheres can easily slip upon elongation (Scheme 2A), and the fracture energies of these films are < 10 MJ/m^3 (Table 3). Thus, highly-crosslinked microspheres, wherein the average chain length for the microspheres is short, should be easily fractured. This notion is supported by the low fracture strain of e.g. BM-D1.3 (~86%) (*cf.* Table 3).

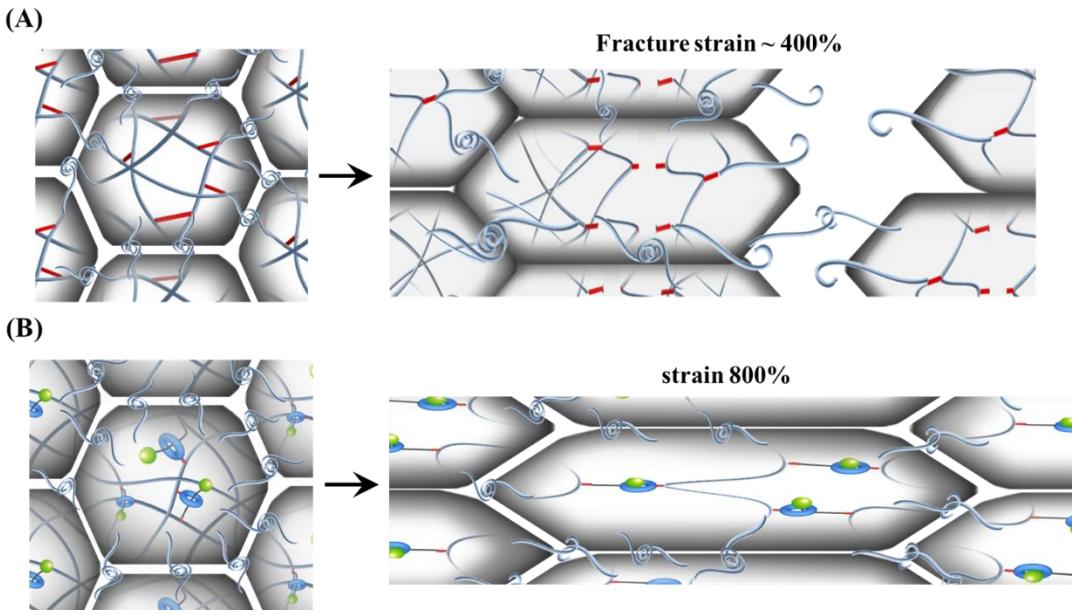

Scheme 2. Illustration of thin films generated from (A) DVB-crosslinked microspheres (BM-D0.05), and (B) **RC**-crosslinked microspheres (BM-R0.05).

Table 3. Characterization of all BM-R*X* and BM-D*X* films investigated in this study.

	Crosslinker	Young's modulus	Fracture strain	Fracture stress	Fracture energy
	[mol%]	[%]	[%]	[MPa]	[MJ/m^3]
BM	0	0.031	489	1.2	4.0
BM-D0.05	0.05	0.075	425	2.8	7.1
BM-D0.45	0.45	0.066	369	4.0	10
BM-D1.3	1.30	0.12	86	2.2	1.5
BM-R0.03	0.03	0.064	572	4.1	13.5
BM-R0.05	0.05	0.043	885	4.5	19.6
BM-R0.07	0.07	0.032	622	2.7	10.5
BM-R0.1	0.1	0.09	360	2.7	7.9
BM-R0.5	0.5	0.048	350	3.0	6.0

In contrast, microspheres with low levels of crosslinking by **RC**, such as BM-R0.05, reveal increased strength and fracture strain (Scheme 2B). This result should be interpreted under

consideration of two points: i) the surface structures, i.e., microspheres with lower degrees of crosslinking should be strongly entangled with adjacent microspheres (Scheme 2A); ii) the effect of stress relaxation in each microsphere that originates from the flexibility of the crosslinking points, which is well known for bulk materials.[7] This effect also affects the fracture energy of the resulting films. Indeed, the fracture energy of films of **RC**-crosslinked microspheres is higher than those of BM and BM-D films (BM-R0.05: ~19.6 MJ/m^3; BM-D0.05: ~7.1 MJ/m^3), even though the mol% of crosslinker is identical in both cases.

To obtain tougher latex films, the author focused on the effect of annealing on the films. Figure 9(A)(B) show fracture energy of the BM-H*X* (denoted as BM-H*X*; B = ~40 mol% BA; M = ~60 mol% MMA; H = HDD; *X* = mol% HDD) and BM-R*X* latex films as a function of the annealing time. All of the annealing latex films showed increased the fracture energy, and the effects of thermal annealing was more effective for latex films prepared from particles crosslinked with **RC** than for latex films prepared from particles crosslinked with HDD and without crosslinkers.

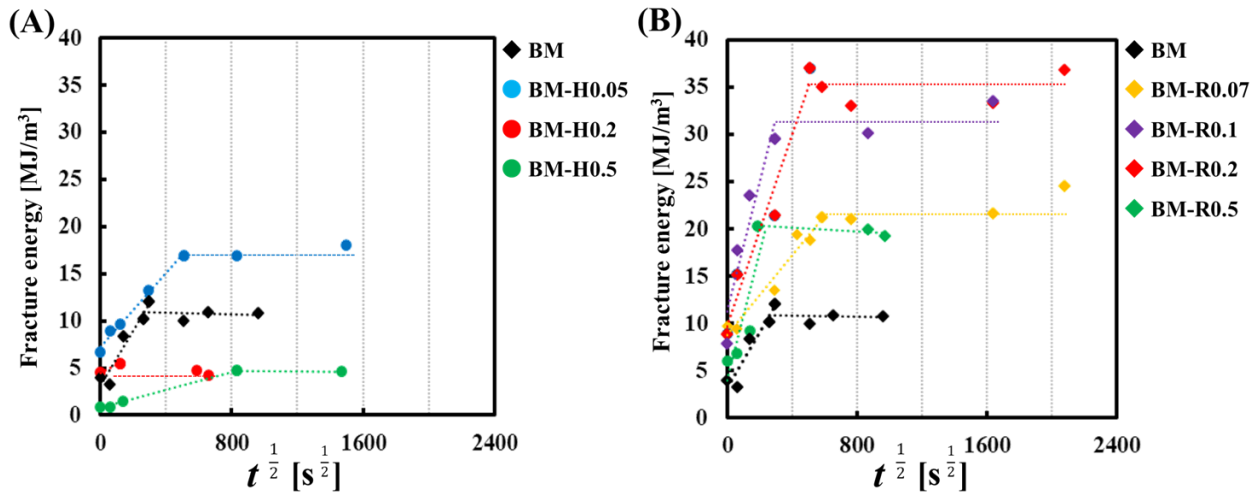

Figure 9. Fracture energy versus the square root of the annealing time. (A) BM-H*X* films (B) BM-R*X* films. The film thickness was ~0.20 mm in all cases.

Although there are still several unresolved issues, including irreversible elastic deformation and surface modification, that need to be addressed for the further development of elastomer microspheres as functional materials, the present results offer access to tough bulk films of

crosslinked microspheres, which represents an important first step towards the next generation of such advanced materials.

3.4. Conclusions

In conclusion, rotaxane-crosslinked elastomer microspheres afford mechanically strong and flexible films by simply evaporating water from their dispersions, even though these microspheres are not crosslinked with supramolecules between the microspheres. The results of this study should find new applications for such films as coatings and adhesives, as well as in the areas of medicine and cosmetics, where the minimization of impurities is desirable.

3.5. References

[1] H. Kawaguchi. Functional polymer microspheres, *Prog. Polym. Sci.*, *25*, 1171-1210, **2000**.

[2] M. Naito, T. Ishii, A. Matsumoto, K. Miyata, Y. Miyahara, K. Kataoka. A Phenylboronate-Functionalized Polyion Complex Micelle for ATP‐Triggered Release of siRNA, *Angew. Chem*., *51*, 10751-10755, **2012**.

[3] L. Nuhn, S. Tomcin, K. Miyata, V. Mail nder, K. Landfester, K. Kataoka, R. Zentel. Size-Dependent Knockdown Potential of siRNA-Loaded Cationic Nanohydrogel Particles, *Biomacromolecules*, *15*, 4111-4121, **2014**.

[4] A. F. Routh, W. B. Russel. A Process Model for Latex Film Formation: Limiting Regimes for Individual Driving Forces, *Langmuir*, *15*, 7762-7773, **1999**.

[5] A. F. Routh, W. B. Russel. Deformation Mechanisms during Latex Film Formation: Experimental Evidence, *Ind. Eng. Chem. Res*., *40*, 4302-4308, **2001**.

[6] E. Carretti, R. Giorgi, D. Berti, P. Baglioni. Oil-in-Water Nanocontainers as Low Environmental Impact Cleaning Tools for Works of Art: Two Case Studies, *Langmuir*, *23*, 6396-6403, **2007**.

[7] D. Kuscer, O. Noshchenko, H. Ur i , B. Mali . Piezoelectric Properties of Ink‐Jet‐Printed Lead Zirconate Titanate Thick Films Confirmed by Piezoresponse Force Microscopy, *J. Am. Ceram. Soc*., *96*, 2714-2717, **2013**.

[8] A. F. Routh. Drying of thin colloidal films, *Rep. Prog. Phys*., 76, 46603, **2013**.

[9] A. Zosel. Mechanical properties of films from polymer latices, *Polym. Adv. Technol*., *6*, 263-269, **1995**.

[10] J. W. Taylor, M. A. Winnik. Functional latex and thermoset latex films, *J. Coat. Technol. Res.*, *1*, 163-190, **2004**.

[11] J. C. Ramirez, M. E. Trevino, J. H. Ordonez, J. Macossay. Hydrolysis of Dimethyl Meta-Isopropenylbenzyl Isocyanate (TMI) and Colloidal Stability of Latexes During Storage: Effect of pH, *J. Macromol. Sci. Phys.*, *51*, 767-776, **2012**.

[12] T. Lü, D. Qi, D. Zhang, Q. Liu, H. Zhao. Fabrication of self-cross-linking fluorinated polyacrylate latex particles with core-shell structure and film properties, *React. Funct. Polym.*, *104*, 9-14, **2016**.

[13] Y. Delaviz, H. W. Gibson. Macrocyclic polymers. 2. Synthesis of poly(amide crown ethers) based on bis(5-carboxy-1,3-phenylene)-32-crown-10. Network formation through threading, *Macromolecules*, *25*, 4859-4862, **1992**.

[14] Y. Okumura, K. Ito. The Polyrotaxane Gel: A Topological Gel by Figure-of-Eight Cross-links, *Adv. Mater.*, *13*, 485-487, **2001**.

[15] T. Oku, Y. Furusho, T. Takata. A Concept for Recyclable Cross-Linked Polymers: Topologically Networked Polyrotaxane Capable of Undergoing Reversible Assembly and Disassembly, *Angew. Chem. Int. Ed.*, *43*, 966-969, **2004**.

[16] K. Ito. Novel Cross-Linking Concept of Polymer Network: Synthesis, Structure, and Properties of Slide-Ring Gels with Freely Movable Junctions, *Polym. J*., *39*, 489-499, **2007**.

[17] J. Sawada, D. Aoki, S. Uchida, H. Otsuka, T. Takata. Synthesis of Vinylic Macromolecular Rotaxane Cross-Linkers Endowing Network Polymers with Toughness, *ACS Macro Lett.*, 4, 598-601, **2015**.

[18] A. B. Imran, K. Esaki, H. Gotoh, T. Seki, K. Ito, Y. Sakai, Y. Takeoka. Extremely stretchable thermosensitive hydrogels by introducing slide-ring polyrotaxane cross-linkers and ionic groups into the polymer network, *Nat. Commun*, *5*, 5124-5132, **2014**.

[19] J. Sawada, D. Aoki, M. Kuzume, K. Nakazono, S. Uchida, H. Otsuka, T. Takata. A vinylic rotaxane cross-linker for toughened network polymers from the radical polymerization of vinyl monomers†, *Polym. Chem.*, 8, 1878-1881, **2017**.

[20] M. Antonietti, K. Landfester. Polyreactions in miniemulsions, *Prog. Polym. Sci.*, *27*, 689-757, **2002**.

[21] J. M. Asua. Miniemulsion polymerization, *Prog. Polym. Sci*., *27*, 1283-1346, **2002**.
[22] S. Pi arra, A. Fidalgo, A. Fedorov, J. M. G. Martinho, J. P. S. Farinha. Smart Polymer Nanoparticles for High-Performance Water-Borne Coatings, *Langmuir*., *30*, 12345-12353, **2014**.
[23] A. Zosel, G. Ley. Influence of crosslinking on structure, mechanical properties, and strength of latex films, *Macromolecules*, 26, 2222-2227, **1993**.

4. Summary

In this thesis, the mechanical properties of latex films prepared from elastomer microspheres were investigated and the correlation between their nanostructures and mechanical properties was examined. Firstly, the relationship between the nanostructure of the latex films and their mechanical properties was investigated using various latex microspheres with different glass-transition temperatures (T_g); the latter can be tuned by changing the mixing ratio of butyl acrylate and methyl methacrylate monomers during the preparation of the microspheres. These latex microspheres exhibited different minimum film-formation temperatures (MFFTs) during the preparation of the latex films. This parameter is one of the key factors that controls the degree of latex-microsphere deformation, which is strongly correlated to the macroscopic mechanical strength of the latex films. The results of this investigation into the (nano)structures of latex films by microscopy and scattering techniques as well as by an examination of their mechanical strength revealed that the toughness of such latex films is intimately correlated to the interfacial thickness between microspheres. Secondly, it was revealed that rotaxane-crosslinked elastomer microspheres allow the production of latex films, obtained from the evaporation of microsphere dispersions, with desirable mechanical and elongation properties, in spite of fact that these microspheres are not crosslinked with any crosslinker between neighboring microspheres.

Latex films are well-established materials that are already industrially mass-produced and have found numerous applications in every-day life. On the other hand, latex films obtained from aqueous synthetic latex solutions exhibit significantly lower mechanical strength than films obtained from organic solutions. In order to increase the mechanical properties of such latex films obtained from aqueous synthetic latex solutions, additives such as photo-polymerization initiators have been introduced during the film formation, which is based on the concept that impurities need to be introduced to improve the strength of the latex films. The findings of this thesis can thus be expected to promote the development of safer manufacturing methods for tougher latex films in the near future.

List of Publicatons

1. **Seina Hiroshige,** Haruka Minato, Yuichiro Nishizawa, Yuma Sasaki, Takuma Kureha, Mitsuhiro Shibayama, Kazuya, Uenishi, Toshikazu Takata, Daisuke Suzuki
"Temperature-dependent Relationship between the Structure and Mechanical Strength of Volatile Organic Compound-free"
Polymer Journal**,** *in press* (**2020**).
DOI: https://doi.org/10.1038/s41428-020-00406-6

2. **Seina Hiroshige**, Takuma Kureha, Daichi Aoki, Jun Sawada, Daisuke Aoki, Toshikazu Takata*, and Daisuke Suzuki*:
"Formation of Tough Films by Evaporation of Water from Dispersions of Elastomer Microspheres Crosslinked with Rotaxane Supramolecules"
Chemistry - A European Journal, Wiley-VCH, 23, pp8405-8408 (**2017**)
DOI: https://doi.org/10.1002/chem.201702077

3. **Seina Hiroshige**, Jun Sawada, Daisuke Aoki, Toshikazu Takata Daisuke Suzuki:
"Investigation of mechanical properties of latex films prepared from poly (butyl acrylate-*co*-methyl methacrylate) microspheres crosslinked with rotaxane"
Nihon Reoroji Gakkaishi, *47*, pp51-54 (**2019**). (written in Japanese)
DOI: 10.1678/rheology.47.51

Other Publicatons

1. Takuma Kureha, **Seina Hiroshige**, Shusuke Matsui, and Daisuke Suzuki*:
"Water-immiscible bioinert coatings and film formation from aqueous dispersions of poly(2-methoxyethyl acrylate) microspheres"
Colloids and Surfaces B: Biointerfaces, Elsevier, 155, pp166-172 (**2017**)
DOI: https://doi.org/10.1016/j.colsurfb.2017.04.001

2. Shusuke Matsui, Takuma Kureha, **Seina Hiroshige**, Mikihiro Shibata, Takayuki Uchihashi* and Daisuke Suzuki*:
"Fast Adsorption of Soft Hydrogel Microspheres on Solid Surfaces in Aqueous Solution"
Angewandte Chemie International Edition, Wiley-VCH, 56, pp1-5 (**2017**)
DOI: 10.1002/anie.201705808

3. Takuma Kureha, Daichi Aoki, **Seina Hiroshige**, Keisuke Iijima, Daisuke Aoki, Toshikazu Takata* and Daisuke Suzuki*:
"Decoupled Thermo- and pH-responsive Hydrogel Microspheres Cross-linked by Rotaxane Networks"
Angewandte Chemie International Edition, Wiley-VCH, pp15393-15396 (**2017**)
DOI: 10.1002/anie.201709633 and 10.1002/ange.201709633

4. Haruka Minato, Masaya Takizawa, **Seina Hiroshige**, Daisuke Suzuki:

"Effect of Charge Groups Immobilized in Hydrogel Microspheres during the Evaporation of Aqueous Sessile Droplets"

Langmuir*, *35, pp10412-10423 **(2019).**

DOI: https://doi.org/10.1021/acs.langmuir.9b01933

5. Takuma Kureha, **Seina Hiroshige**, Daisuke Suzuki, Jun Sawada, Daisuke Aoki, Toshikazu Takata, Mitsuhiro Shibayama:

"Quantification for the Mixing of Polymers on Microspheres in Water-borne Latex Films"

Langmuir, 36, pp4855-4862 (2020).

DOI: https://doi.org/10.1021/acs.langmuir.0c00612

Reviews

1. 広重聖奈、松井秀介、鈴木大介

「進化するコーティング技術 ― コーティング材料の「今まで」と「これから」」

化学、第73巻、第2号、pp64-65 (2018).

Oral Presentation (International conference)

1. ○**Seina Hiroshige**, Jun Sawada, Daisuke Aoki, Toshikazu Takata, Daisuke Suzuki:

"Formation of Tough Latex Films of Polymeric Microspheres Crosslinked with Rotaxane"

ACS Fall 2019 National Meeting (San Diego, USA) August 29(2019) Oral (COLL 711)

Oral Presentation (National conference)

1. ○広重聖奈、呉羽拓真、青木大地、澤田隼、青木大輔、高田十志和、鈴木大介

"可動な架橋点を有するエラストマー微粒子の創製及びフィルム形成"

第 65 回高分子討論会、神奈川大学、9 月 15 日(2016) 、発表番号 2T16

2. ○松井秀介、呉羽拓真、広重聖奈、柴田幹大、内橋貴之、鈴木大介

"高速 AFM による高分子微粒子の固液界面上における動的挙動のリアルタイム可視化"

新学術領域研究「動的秩序と機能」第 3 回若手研究会、片山津温泉加賀観光ホテル、石川、10 月 12 日(2016)、発表番号 1

3. ○広重聖奈、呉羽拓真、青木大地、澤田隼、青木大輔、高田十志和、鈴木大介

"ロタキサン架橋剤を導入したエラストマー微粒子の創製と強靭な透明フィルムへの応用"第 19 回高分子ミクロスフェア討論会、3-03A、千葉大学、11 月 9 日(2016)、発表番号 3-03A

4. ○広重聖奈、呉羽拓真、青木大地、澤田隼、青木大輔、高田十志和、鈴木大介

"ロタキサン架橋剤を導入したエラストマー微粒子の合成と微粒子集積フィルムへの応用"第 28 回高分子ゲル研究討論会、東京大学、1 月 17 日(2017)、発表番号 22

5. ○広重聖奈、呉羽拓真、青木大地、澤田隼、青木大輔、高田十志和、鈴木大介

"ロタキサン架橋を施したエラストマー微粒子の合成と強くしなやかなフィルムへの応用"

日本化学会 第 97 春季年会、慶応義塾大学、3 月 18 日(2017)、発表番号 3B5-40

6. ○松井秀介、呉羽拓真、**広重聖奈**、柴田幹大、内橋貴之、鈴木大介
“高速原子間力顕微鏡による高分子微粒子の固体表面への吸着挙動のリアルタイム評価”
第 68 回コロイドおよび界面化学討論会、神戸大学、兵庫、9 月 6 日(2017)、発表番号 1F47

7. ○**広重聖奈**、呉羽拓真、澤田隼、青木大輔、高田十志和、鈴木大介
“超分子架橋を施したアクリレート系微粒子分散液の乾燥による強靭なフィルムの形成”
第 68 回コロイドおよび界面化学討論会、神戸大学、兵庫、9 月 8 日(2017)、発表番号 3D27

8. ○**広重聖奈**、呉羽拓真、澤田隼、青木大輔、高田十志和、鈴木大介
“Formation of Tough Films by Evaporation of Water from Dispersions of Elastomer microspheres Crosslinked with Rotaxane Structure”
第 27 回日本 MRS 年次大会、横浜市開港記念会館、神奈川、12 月 5 日(2017)、
発表番号 I-O5-017
※ 奨励賞

9. ○**広重聖奈**、呉羽拓真、澤田隼、青木大輔、高田十志和、鈴木大介
“Design and Synthesis of Rotaxane Crosslinked Microspheres and their application”
第 67 回高分子学会年次大会、名古屋国際会議場、愛知、5 月 24 日(2018)、発表番号 2M14

10. ○**広重聖奈**、澤田隼、青木大輔、高田十志和、鈴木大介
“ロタキサン架橋した高分子微粒子の創製とフィルム形成”
第 20 回高分子ミクロスフェア討論会、岡山大学、岡山、11 月 15 日(2018)、発表番号 2-08A
※ 学生優秀発表賞

11. ○**広重聖奈**、澤田隼、青木大輔、高田十志和、鈴木大介
“ロタキサン架橋を施したエラストマー微粒子の創製とフィルムの形成”
第 29 回エラストマー討論会、名古屋市中小企業振興会館、愛知、11 月 29 日(2018)、
発表番号 D-1
※ 若手優秀発表賞

12. ○**広重聖奈**、澤田隼、青木大輔、高田十志和、鈴木大介
“ロタキサン架橋微粒子の創製とラテックスフィルムの力学的特性評価”
第 30 回高分子ゲル研究討論会、東京工業大学、東京、1 月 16 日(2019)、発表番号 8
※ 優秀演題賞

13. ○湊遥香、滝沢優哉、**広重聖奈**、鈴木大介
“気水表面において織り成す高分子電解質ゲル微粒子の特異な自己組織化挙動”
第 68 回高分子討論会、福井大学、福井、9 月 25 日(2019)、発表番号 1J10

14. ○岩瀬健吾、**広重聖奈**、澤田隼、青木大輔、高田十志和、鈴木大介
“ロタキサン架橋を施したエラストマー微粒子から成るラテックスフィルムの力学特性に与える化学種の影響”
第 50 回中部化学関係学協会支部連合秋季大会、信州大学松本キャンパス、長野、
11 月 10 (2019)、発表番号 2L14

15. ○湊遥香、滝沢優哉、**広重聖奈**、鈴木大介
“気水界面における高分子電解質ゲル微粒子がみせる自己組織化挙動”

第 29 回日本 MRS 年次大会、横浜情報文化センター、神奈川、11 月 29 日(2019)、
発表番号 O-O29-004

16. ○**広重聖奈**、澤田隼、青木大輔、高田十志和、鈴木大介
"ロタキサン架橋を施した強靭な微粒子フィルムの形成"
第 29 回日本 MRS 年次大会、横浜情報文化センター、神奈川、11 月 29 日(2019)、
発表番号 O-O29-002

17. ○呉羽拓真、**広重聖奈**、鈴木大介、澤田隼、青木大輔、高田十志和、柴山充弘
"放射光 X 線散乱法による水系ラテックスフィルムのナノ構造解析"
第 69 回高分子討論会、オンライン開催、9 月 17 日(2020)、発表番号 2H07

18. ○**広重聖奈**、湊遥香、佐々木悠馬、呉羽拓真、柴山充弘、上西和也、澤田隼、青木大輔、
高田十志和、鈴木大介
"ロタキサン架橋を導入したエラストマー微粒子から成るラテックスフィルムの力学特性評価"
第 69 回高分子討論会、オンライン開催、9 月 16 日(2020)、発表番号 1J08

19. ○佐々木悠馬、**広重聖奈**、澤田隼、青木大輔、高田十志和、鈴木大介
"ロタキサン架橋を施したラテックスフィルムの形成とその力学評価"
第 69 回高分子討論会、オンライン開催、9 月 18 日(2020)、発表番号 3N03

20. ○**広重聖奈**、湊遥香、西澤佑一郎、佐々木悠馬、呉羽拓真、柴山充弘、上西和也、高田十志和、
鈴木大介
"不純物を含まずに形成したラテックスフィルムのナノ構造と力学特性"
2020 年度東海高分子研究会学生発表会、オンライン開催、11 月 7 日(2020)、発表番号 2-19
※ 東海高分子研究会優秀口頭発表賞

21. ○**広重聖奈**、湊遥香、西澤佑一郎、佐々木悠馬、呉羽拓真、柴山充弘、上西和也、高田十志和、
鈴木大介
"アクリレート微粒子から形成される強靭なラテックスフィルムの創製と応用"
第 30 回日本 MRS 年次大会、オンライン開催、12 月 9 日(2020)、発表番号 G-O9-010

Patent

1. 上西和也、新家雄、鈴木大介、**広重聖奈**、澤田隼、青木大輔、高田十志和
「高分子微粒子」、
特願 2016-163014、出願日 8 月 23 日 (2016)、特開 2018-030928、公開日 3 月 1 日 (2018)

2. 上西和也、新家雄、岡松隆裕、**広重聖奈**、鈴木大介、澤田隼、青木大輔、高田十志和
「高分子微粒子」、
特願 2017-228835、出願日 11 月 29 日(2017)、特開 2019-099607、公開日 6 月 24 日 (2019)

3. 鈴木大介、高田十志和、**広重聖奈**、佐々木悠馬、大日方秀平、大倉滉生、脇屋武司
「成形体及び成形体の製造方法」、
特願 2020-105606、出願日 6 月 18 日 (2020)

Awards

1. 第161回東海高分子研究会講演会 学生研究奨励賞 (2017年)
2. 第27回日本MRS年次大会 奨励賞 (2017年)
3. 平成29年度応用分子化学ユニット修士論文発表会 日本化学会東海支部長賞 (2018年)
4. 第67回高分子学会年次大会 高分子学会優秀ポスター賞 (2018年)
5. 第20回高分子ミクロスフェア討論会 学生優秀発表賞 (2018年)
6. 第29回エラストマー討論会 若手優秀発表賞 (2018年)
7. 第30回高分子ゲル研究討論会 優秀演題賞 (2019年)
8. 2020年度東海高分子研究会学生発表会 東海高分子研究会優秀口頭発表賞